


Optimal estimation of matter-field coupling strength in the dipole approximation

József Zsolt Bernád,^{*} Claudio Sanavio,[†] and André Xuereb
Department of Physics, University of Malta, Msida MSD 2080, Malta

 (Received 21 December 2018; published 12 June 2019)

This paper is devoted to the study of the Bayesian-inference approach in the context of estimating the dipole coupling strength in matter-field interactions. In particular, we consider the simplest model of a two-level system interacting with a single mode of the radiation field. Our estimation strategy is based on the emerging state of the two-level system, whereas we determine both the minimum mean-square error and maximum likelihood estimators for uniform and Gaussian prior probability density functions. In the case of the maximum likelihood estimator, we develop a mathematical method which extends the already existing approaches to the variational problem of the average cost function. We demonstrate that long interaction times, large initial mean photon numbers, and nonzero detuning between two-level system transition and the frequency of the electromagnetic field mode have a *deleterious* effect on the optimality of the estimation scenario. We also present several cases where the estimation process is inconclusive, despite many ideal conditions being met.

DOI: [10.1103/PhysRevA.99.062106](https://doi.org/10.1103/PhysRevA.99.062106)

I. INTRODUCTION

Measurements of physical systems with complete description can be anticipated and the problem of prediction is the forward problem. The inverse problem consists of the estimation of physical parameters using the available measurement data [1]. In quantum mechanics, we seek to estimate the physical parameters governing the evolution of a density matrix from measurements made on part of the system. Against this background, the problem of optimal measurements in quantum systems has been a major focus since the beginning of quantum estimation theory [2,3]. The criterion of optimality is defined through the cost experienced upon making errors in the estimates. This measure is formulated by means of the so-called cost function of the estimates and the true values of the parameters. The optimum strategy attempts to find that positive-operator valued measure (POVM) which minimizes the average cost functional calculated with the help of the cost function, the density matrix, and the POVM. The rigorous mathematical meaning of the average cost functional and conditions under which solutions of the optimization problem exist were thoroughly investigated by Holevo [4]. In this context, a particularly convenient approach is the Bayesian-inference method, where one assumes that the true values of the physical parameters are random variables with a given prior probability density function (PDF) [5].

In this paper, we continue our investigations of the Bayesian-inference approach with a focus on one-parameter estimation scenarios in order to gain a better insight into the properties of the estimators [6]. We shall consider the problem of estimating the dipole coupling of matter-field interactions [7]. Because of the widespread applications of these interactions in, e.g., quantum communication [8], a

precise determination of the dipole coupling has increasing technological, as well as fundamental, relevance. While quantum electrodynamics gives a straightforward recipe for calculating this matter-field coupling [9], experimental limitations on precision inherently introduce probabilistic variations in this parameter. Typically, the dipole coupling varies along the trajectory of the moving atom due to the mode structure in the cavity [10,11] or in case of trapped atoms due to the temperature-induced position probability distribution [12]. The experiments usually determine an effective dipole coupling by integrating over the variations of the coupling strength. Another way to gain some knowledge is to perform measurements on the physical system and obtain data, from which the value of the effective dipole coupling can be inferred. In the context of the Bayesian-inference approach, one may even obtain the optimum estimators. Here in this paper, we determine not only the minimum mean-square error estimator for a Gaussian PDF [6], but we consider also a uniform prior PDF. These type of *a priori* PDF are going to be applied also in the determination of optimum maximum likelihood estimator. The method presented in Ref. [6] and elaborated upon here should be distinguished from the quantum Fisher information approach [13], which has also been successfully applied to systems with matter-field interactions [14,15].

In our model, two-level systems (TLSs) transit through a cavity supporting a single mode of the radiation field and are then measured. We trace out the single-mode radiation field and concentrate on the resulting density matrix, subject to the quantum estimation procedure. Spontaneous decay of the TLS is also taken into account. In the case of the minimum mean-square error estimator, we invoke the method applied in our previous work [6], demonstrating that the resulting optimal detection strategy can be related to implementable measurement setups in experimentally relevant situations. The problem of determining the maximum likelihood estimator is centered around the resolution of identity and integration with respect to an operator valued measure; see Dobrakov's

^{*}zsolt.bernad@um.edu.mt

[†]claudio.sanavio@um.edu.mt

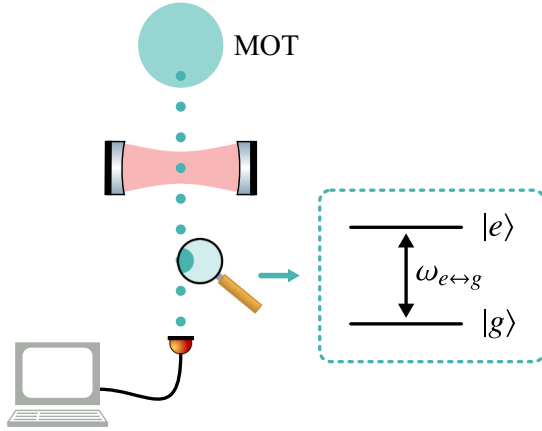


FIG. 1. Schematic representation of a quantum estimation scenario based on cavity QED. The atoms (gray dots) implementing the two-level systems are captured from a background gas by a magneto-optical trap and loaded into an optical conveyor belt [19]. The atoms move with the help of the conveyor belt into and out of the cavity and toward a detector. The transition frequency of the atom is $\omega_{e\leftrightarrow g}$. Further details about the scheme are in the text.

integral in Ref. [16]. Because of our motivations being rooted in physics, we choose to avoid generalized theories of the Lebesgue integral [17], instead making a simple ansatz for the POVM with the help of square-integrable functions. This construction allows us to determine the maximum likelihood estimators for both the uniform and Gaussian prior PDF and offers a mathematical tool for the maximum likelihood estimation strategy. Whereas estimating the phases of states, displacement parameters, wave vectors, and coherent signal amplitudes involves solving the equations for the optimum strategy involving the risk operator [4], here we focus directly on the extrema of the average cost function, which determine the optimum POVMs. We will present numerical calculations of the average cost functions, the average estimates, and lower bounds of the mean-squared error of the obtained biased estimators.

This paper is organized as follows. In Sec. II, we discuss the model and determine the state of the TLS following its interaction with the single-mode radiation field. Spontaneous decay of the TLS is also considered. In Sec. III, we recapitulate some basic facts about quantum estimation theory and introduce the formalism used throughout the paper. We then address the problem of determining the minimum mean-square error estimator in Sec. IV. In Sec. V, maximum likelihood estimators are discussed. Finally, we discuss our work and draw our conclusions in Sec. VI.

II. MODEL

In this section, we discuss a cavity QED model consisting of a TLS interacting with a single-mode electromagnetic cavity. The TLS, generally implemented as a flying atom, is injected into the cavity and emerges from the cavity and is detected after interacting with the electromagnetic field. The setup, illustrated in Fig. 1, is one of the best suited for our estimation procedure, because it is under exquisite

experimental control [7,18,19] and because it allows repeated measurements to be made using several TLSs interacting sequentially with the field. In fact, this is a very important point in estimation scenarios because the use of N independent and identical systems reduces the lower bound of the estimation accuracy by a factor of N^{-1} [2]. Therefore, it is assumed that before each TLS enters the cavity, the single-mode field is always reset to the same initial state. The state of each TLS entering the cavity is also assumed to be the same. In practice, the controlled motion of an atom into and out of the cavity may be realized using an optical conveyor belt [19], i.e., a moving dipole trap, into which atoms are loaded from a magneto-optical trap. In our discussion, we present the solution to this elementary model and determine the state of the atom by tracing out the state of the electromagnetic field. The optimal estimator for the matter-field coupling will be subsequently determined for each presented estimation scenario.

Let us consider a TLS with ground state $|g\rangle$ and excited state $|e\rangle$. Cavity leakage and spontaneous decay of the TLS are present; nonetheless, it is assumed in most parts of the presented work that the coupling strength of the matter-field interaction is much larger than the damping rate of the two decoherence sources. Therefore, the joint TLS-field state during the matter-field interaction time can effectively be described by a purely unitary evolution. In the dipole and rotating-wave approximations, the Hamiltonian in the time-independent interaction picture reads [20,21] ($\hbar = 1$)

$$\hat{H} = \frac{\Delta}{2}\hat{\sigma}_z + g(\hat{a}\hat{\sigma}_+ + \hat{a}^\dagger\hat{\sigma}_-), \quad (1)$$

where $\hat{\sigma}_z = |e\rangle\langle e| - |g\rangle\langle g|$, $\hat{\sigma}_+ = |e\rangle\langle g|$ is the raising operator, and $\hat{\sigma}_- = |g\rangle\langle e|$ is the lowering operator. \hat{a} and \hat{a}^\dagger are the annihilation and creation operators of the field mode. $\Delta = \omega_{e\leftrightarrow g} - \omega_c$ is the detuning between the cavity field mode resonance frequency ω_c and the TLS transition frequency $\omega_{e\leftrightarrow g}$. Finally, g is the dipole coupling strength, which involves the normalized mode function of the single-mode radiation field and the transition dipole moment between $|g\rangle$ and $|e\rangle$.

We suppose that at $t = 0$ there are no correlations between the field and the TLS. Furthermore, we set the TLS to be initially in the excited state. Thus, our general initial quantum state reads

$$|\psi(t=0)\rangle = |e\rangle \otimes \sum_{n=0}^{\infty} a_n |n\rangle, \quad (2)$$

where $|n\rangle$ ($n \in \mathbb{N}_0$) are the normalized photon number states and $\sum_{n=0}^{\infty} |a_n|^2 = 1$. The time evolution is governed by the Schrödinger equation acting on the initial state (2) yields

$$|\psi(t)\rangle = \sum_{n=1}^{\infty} c_{e,n-1}(t)|e, n-1\rangle + c_{g,n}(t)|g, n\rangle, \quad (3)$$

where [9]

$$c_{e,n-1}(t) = e^{-i\frac{\Delta t}{2}} \left[\cos(\lambda_n t) + i\frac{\Delta}{2\lambda_n} \sin(\lambda_n t) \right] a_{n-1},$$

$$c_{g,n}(t) = -ie^{i\frac{\Delta t}{2}} \frac{g\sqrt{n}}{\lambda_n} \sin(\lambda_n t) a_{n-1},$$

and where $\lambda_n = \sqrt{\Delta^2/4 + g^2 n}$ is the effective Rabi frequency. The state of the TLS upon emerging from the cavity is obtained by tracing out the state of the field,

$$\begin{aligned} \hat{\rho}(g, t) &= \text{Tr}_F\{|\psi(t)\rangle\langle\psi(t)|\} \\ &= \begin{bmatrix} a_{ee}(t) & a_{eg}(t) \\ a_{eg}^*(t) & 1 - a_{ee}(t) \end{bmatrix}, \end{aligned} \quad (4)$$

where

$$a_{ee}(t) = \sum_{n=1}^{\infty} |a_{n-1}|^2 \left[\cos^2(\lambda_n t) + \frac{\Delta^2}{4\lambda_n^2} \sin^2(\lambda_n t) \right], \quad (5)$$

$$\begin{aligned} a_{eg}(t) &= \sum_{n=1}^{\infty} a_n a_{n-1}^* \left[\cos(\lambda_{n+1} t) + i \frac{\Delta}{2\lambda_{n+1}} \sin(\lambda_{n+1} t) \right] \\ &\quad \times \frac{ig\sqrt{n}}{\lambda_n} \sin(\lambda_n t) e^{-i\Delta t}. \end{aligned} \quad (6)$$

In the next stage of the experiment, the TLS flies from the cavity to the detector. During this time, spontaneous emission may occur. We include this effect in our calculations by using a simple Markovian description

$$\frac{d\hat{\rho}}{dt} = \frac{\gamma}{2} (2\hat{\sigma}_- \hat{\rho} \hat{\sigma}_+ - \hat{\sigma}_+ \hat{\sigma}_- \hat{\rho} - \hat{\rho} \hat{\sigma}_+ \hat{\sigma}_-), \quad (7)$$

where γ is the spontaneous emission rate of the TLS. Equation (7) is written in the frame rotating at the resonance frequency of the TLS. Two characteristic times enter our discussion: τ_c , the duration of the matter-field interaction in the cavity, and τ_f , the flying time from the cavity to the detector. The solution in Eq. (4) at $t = \tau_c$ can be considered as the initial condition for Eq. (7). Thus, the state of the TLS reaching the detector is

$$\hat{\rho}(g) = \begin{bmatrix} a_{ee}(g, \tau_c) e^{-\gamma\tau_f} & a_{eg}(g, \tau_c) e^{-\gamma\tau_f/2} \\ a_{eg}^*(g, \tau_c) e^{-\gamma\tau_f/2} & 1 - a_{ee}(g, \tau_c) e^{-\gamma\tau_f} \end{bmatrix}. \quad (8)$$

Equation (8) yields a complete description of our setup and it applies to all the possible initial conditions of the field. A major theme of our subsequent discussion will be the analysis of Eq. (8) in the context of quantum estimation theory, where we shall seek optimal estimators for the coupling strength g .

III. QUANTUM ESTIMATION THEORY

In this section, we summarize basic facts about parameter estimation in quantum theory which are relevant for our subsequent discussion and which have been reviewed in detail by Helstrom [2]. In particular, we summarize the methods and the concept behind them in order to provide an optimal estimation for the dipole coupling strength g from the density matrix (8).

The observational strategy for estimating g , a real number, can be expressed as a search for a POVM defined on the set $\Theta \subseteq \mathbb{R}$ of all possible values of g . The elements of the POVM represent the measurements to be performed on the TLS, which result in estimates \tilde{g} of g , where \tilde{g} is a random variable. The probability that it lies in a particular region Δ of the set Θ , provided that the true value of the estimated dipole coupling is g , reads

$$P(\tilde{g} \in \Delta | g) = \text{Tr}\{\hat{\rho}(g) \hat{\Pi}(\Delta)\}. \quad (9)$$

$\hat{\Pi}(\Delta)$ is an element of the POVM which is a mapping of regions $\Delta \subset \Theta$ into positive semidefinite operators on the Hilbert space \mathbb{C}^2 of the TLS with the following properties:

$$0 \leq \hat{\Pi}(\Delta) \leq \hat{I}, \quad \hat{\Pi}(\emptyset) = \hat{0}, \quad \text{and} \quad \hat{\Pi}(\Theta) = \hat{I}, \quad (10)$$

where \emptyset stands for the empty set and $\hat{0}$ and \hat{I} are the null and identity operators. Furthermore, we suppose that POVM elements on compact intervals Δ can be written as integrals with the help of the infinitesimal operators $d\hat{\Pi}(g)$, thus yielding

$$\hat{\Pi}(\Delta) = \int_{\Delta} d\hat{\Pi}(g) \quad \text{and} \quad \int_{\Theta} d\hat{\Pi}(g) = \hat{I}. \quad (11)$$

The conditional PDF of the estimate \tilde{g} is given by

$$p(\tilde{g}|g)d\tilde{g} = \text{Tr}\{\hat{\rho}(g)d\hat{\Pi}(\tilde{g})\}, \quad (12)$$

where $d\tilde{g}$ represents an infinitesimal compact interval in the set Θ .

The *Bayesian formulation* of the estimation problem seeks for the best estimator which minimizes the average cost of its application. In order to solve this estimation problem we have to provide an *a priori* PDF $z(g)$ of g to be estimated and a cost function $C(\tilde{g}, g)$, which assesses the cost of error in the estimate. Now, combining the Bayesian estimation procedure with the strategy represented by the POVM in Eq. (10) and including integral representation in Eq. (11), we obtain for the average cost

$$\bar{C} = \text{Tr} \left\{ \int_{\Theta} dg \int_{\Theta} d\hat{\Pi}(\tilde{g}) z(g) C(\tilde{g}, g) \hat{\rho}(g) \right\}. \quad (13)$$

We are looking for the $d\hat{\Pi}(\tilde{g})$ which minimizes \bar{C} . Our problem has thus been rephrased as a variational problem formulated on the space of all POVMs. In order to solve this problem, one ought to first define $C(\tilde{g}, g)$. In this article, we will employ the frequently used quadratic cost function

$$C(\tilde{g}, g) = (\tilde{g} - g)^2, \quad (14)$$

which leads to the minimum mean-square error (MMSE) estimator, and the δ -valued cost function

$$C(\tilde{g}, g) = -\delta(\tilde{g} - g), \quad (15)$$

which leads to the maximum likelihood (ML) estimator [2].

In the following sections, we will investigate both the MMSE and the ML estimation scenarios for different prior PDF.

IV. MINIMUM MEAN-SQUARE ERROR ESTIMATOR

In the case of the quadratic cost function, there is a more direct way to formulate the variational problem of Eq. (13) [22]. Let us assume that the elements of the POVM are projectors, with the infinitesimal operator

$$d\hat{\Pi}(\tilde{g}) = |\tilde{g}\rangle\langle\tilde{g}|d\tilde{g},$$

where $|\tilde{g}\rangle$ are the eigenstates of the estimator

$$\hat{M} = \int_{\Theta} \tilde{g} d\hat{\Pi}(\tilde{g}) = \int_{\Theta} \tilde{g} |\tilde{g}\rangle\langle\tilde{g}| d\tilde{g}, \quad (16)$$

and here \tilde{g} stands for the all possible values of the estimate. In fact, the most convenient way to think about \hat{M} is to consider

it as an operator to be measured, with its eigenvalues the estimates of g [6]. Furthermore, the Hilbert space is \mathbb{C}^2 in our setup, which means that the POVM has only two projectors as elements, which project onto the eigenstates of \hat{M} . The average cost in Eq. (13), together with Eq. (16), yields

$$\bar{C}[\hat{M}] = \text{Tr} \left\{ \int_{\Theta} z(g) (\hat{M} - g\hat{I})^2 \hat{\rho}(g) dg \right\}. \quad (17)$$

The unique Hermitian operator \hat{M}_{\min} , the MMSE estimator, which minimizes $\bar{C}[\hat{M}]$ is the solution of the operator equation [22]

$$\hat{\Gamma}_0 \hat{M}_{\min} + \hat{M}_{\min} \hat{\Gamma}_0 = 2\hat{\Gamma}_1, \quad (18)$$

where we have introduced the family of operators ($k = 0, 1, 2$):

$$\hat{\Gamma}_k = \int_{\Theta} g^k z(g) \hat{\rho}(g) dg. \quad (19)$$

The solution to Eq. (18) reads

$$\hat{M}_{\min} = 2 \int_0^{\infty} \exp(-\hat{\Gamma}_0 x) \hat{\Gamma}_1 \exp(-\hat{\Gamma}_0 x) dx, \quad (20)$$

and the associated average minimum cost of error for the MMSE estimator is

$$\bar{C}_{\min} = \text{Tr} \{ \hat{\Gamma}_2 - \hat{M}_{\min} \hat{\Gamma}_0 \hat{M}_{\min} \}. \quad (21)$$

In order to gain insight into the structure of \hat{M}_{\min} , let us concentrate on resonant interactions $\Delta = \omega_{e \leftrightarrow g} - \omega_c = 0$. We also consider the initial state of the single-mode field in (2) to be the ground state, $a_0 = 1$. In this case, Eq. (8) reads

$$\hat{\rho}(g) = \begin{bmatrix} \cos^2(g\tau_c) e^{-\gamma\tau_f} & 0 \\ 0 & 1 - \cos^2(g\tau_c) e^{-\gamma\tau_f} \end{bmatrix}. \quad (22)$$

We assume that the random variable g to be estimated is characterized by its mean value g_0 and variance σ^2 . In order to connect these parameters to experimental setups, we start with the position-dependent dipole coupling of the matter-field interaction [9],

$$g(\vec{r}_q) = -\sqrt{\frac{\hbar\omega_c}{2\epsilon_0}} \langle g | \hat{d} | e \rangle \cdot \vec{u}(\vec{r}_q) / \hbar,$$

where \hat{d} is the dipole operator, ϵ_0 is the permittivity of vacuum, and \vec{r}_q is the position vector. The normalized mode function of the single-mode radiation field, $\vec{u}(\vec{r})$, is a solution to the Helmholtz equation and fulfills the Coulomb gauge and the cavity boundary conditions. However, every passing TLS also experiences changes in the dipole coupling due to the waist of the field mode. Experimental studies usually integrate the collected data over the flying time through the cavity and thus obtain an average coupling strength g_0 ; cf., for example, Ref. [11]. This method results also in a variance σ^2 of the measured coupling strength. In the following, we are going to discuss two prior PDFs whose mean values and variances coincide with the values defined here.

A. Gaussian probability density function

In this subsection, we consider $\Theta = \mathbb{R}$ and the prior PDF

$$z(g) = \frac{1}{\sqrt{2\pi\sigma^2}} e^{-\frac{(g-g_0)^2}{2\sigma^2}}, \quad g \in \Theta. \quad (23)$$

As $z(g)$ and the density matrix in Eq. (22) are given, the operators defined in Eq. (19) can be evaluated explicitly, yielding

$$\begin{aligned} \hat{\Gamma}_0 &= \begin{bmatrix} ae^{-\gamma\tau_f} & 0 \\ 0 & 1 - ae^{-\gamma\tau_f} \end{bmatrix}, \\ a &= \frac{1 + e^{-2\sigma^2\tau_c^2} \cos(2g_0\tau_c)}{2}, \\ \hat{\Gamma}_1 &= \begin{bmatrix} be^{-\gamma\tau_f} & 0 \\ 0 & g_0 - be^{-\gamma\tau_f} \end{bmatrix}, \\ b &= \frac{g_0 + e^{-2\sigma^2\tau_c^2} [g_0 \cos(2g_0\tau_c) - 2\sigma^2\tau_c \sin(2g_0\tau_c)]}{2}, \\ \hat{\Gamma}_2 &= \begin{bmatrix} ce^{-\gamma\tau_f} & 0 \\ 0 & g_0^2 + \sigma^2 - ce^{-\gamma\tau_f} \end{bmatrix}, \end{aligned}$$

and

$$\begin{aligned} c &= \frac{(g_0^2 + \sigma^2) [1 + e^{-2\sigma^2\tau_c^2} \cos(2g_0\tau_c)]}{2} \\ &\quad - 2g_0\sigma^2\tau_c e^{-2\sigma^2\tau_c^2} \sin(2g_0\tau_c) \\ &\quad - 2\sigma^4\tau_c^2 e^{-2\sigma^2\tau_c^2} \cos(2g_0\tau_c). \end{aligned}$$

Now, Eq. (20) can be directly calculated and the MMSE estimator reads

$$\hat{M}_{\min} = \begin{bmatrix} \frac{b}{a} & 0 \\ 0 & \frac{g_0 - be^{-\gamma\tau_f}}{1 - ae^{-\gamma\tau_f}} \end{bmatrix}. \quad (24)$$

The average minimum cost of error is

$$\begin{aligned} \bar{C}_{\min} &= g_0^2 + \sigma^2 - \left(\frac{g_0 - be^{-\gamma\tau_f}}{1 - ae^{-\gamma\tau_f}} \right)^2 \\ &\quad - ae^{-\gamma\tau_f} \left[\frac{b^2}{a^2} - \left(\frac{g_0 - be^{-\gamma\tau_f}}{1 - ae^{-\gamma\tau_f}} \right)^2 \right]. \end{aligned}$$

To illustrate the meaning of the MMSE estimator \hat{M}_{\min} and the average minimum cost of error \bar{C}_{\min} , we consider a situation where the experimentalist, based on their prior expectations of the coupling strength g , sets the duration of the matter-field interaction $\tau_c = \pi/(2g_0)$. This reflects the fact that the experimentalist expects the TLS to emit a photon into the field mode and fly toward the detectors in its ground state. This setup yields

$$\hat{M}_{\min} = \begin{bmatrix} g_0 & 0 \\ 0 & g_0 \end{bmatrix}, \quad \bar{C}_{\min} = \sigma^2,$$

which means that the estimates \tilde{g} are always g_0 regardless of the applied projective measurement. Furthermore, the average minimum cost of error is σ^2 . Thus, this scenario simply reinforces prior expectations on the true value of g . Another inconclusive setup would be when $\tau_c = \pi/g_0$, i.e., the experimentalist expects that the TLS will not emit a photon into the field mode.

A much more interesting scenario is when $\tau_c = \pi/(4g_0)$ or in other words the experimentalist expects the TLS to emit a photon with 50% probability. Now, we have

$$\hat{M}_{\min} = \begin{bmatrix} g_0 - \frac{\sigma^2 \pi}{2g_0} e^{-\frac{\pi^2}{8} \frac{\sigma^2}{g_0^2}} & 0 \\ 0 & g_0 + \frac{\sigma^2 \pi}{2g_0} \frac{1}{2e^{\gamma\tau_f} - 1} e^{-\frac{\pi^2}{8} \frac{\sigma^2}{g_0^2}} \end{bmatrix}$$

and

$$\bar{C}_{\min} = \sigma^2 - \frac{\sigma^4 \pi^2}{4g_0^2} \frac{1}{2e^{\gamma\tau_f} - 1} e^{-\frac{\pi^2}{4} \frac{\sigma^2}{g_0^2}}.$$

Measuring the TLS in the excited state results in the estimate

$$\tilde{g} = g_0 - \frac{\sigma^2 \pi}{2g_0} e^{-\frac{\pi^2}{8} \frac{\sigma^2}{g_0^2}},$$

with probability

$$p = \cos^2\left(\frac{\pi}{4} \frac{g}{g_0}\right) e^{-\gamma\tau_f}.$$

The destructive effects of the spontaneous decay are revealed here, because when $\gamma\tau_f \gg 1$ this probability reduces to zero and therefore the measurement cannot obtain the estimate belonging to the excited state of the TLS. When the measurement yields the other outcome, the state is projected onto the ground state of the TLS, and the resulting estimate is

$$\tilde{g} = g_0 + \frac{\sigma^2 \pi}{2g_0} \frac{1}{2e^{\gamma\tau_f} - 1} e^{-\frac{\pi^2}{8} \frac{\sigma^2}{g_0^2}}$$

with probability

$$p = 1 - \cos^2\left(\frac{\pi}{4} \frac{g}{g_0}\right) e^{-\gamma\tau_f}.$$

When $\gamma\tau_f \gg 1$, this result is obtained with certainty, and the resulting estimate is simply g_0 and $\bar{C}_{\min} = \sigma^2$. Again our prior expectations of the true value of g are reinforced. In general, the average estimate is

$$\begin{aligned} E[\tilde{g}|g] &= \text{Tr}\{\hat{M}_{\min}\hat{\rho}(g)\} \\ &= g_0 - \cos\left(\frac{\pi}{2} \frac{g}{g_0}\right) \frac{\sigma^2 \pi}{2g_0} \frac{1}{2e^{\gamma\tau_f} - 1} e^{-\frac{\pi^2}{8} \frac{\sigma^2}{g_0^2}}, \end{aligned}$$

which is conditioned on the true value of g . Performing several measurements with identical TLSs yields an average estimate from which one may deduce the value of g . When the standard deviation σ of the prior PDF is set very large compared to the prior mean $g_0 \ll \sigma$, we allow the true value of g to be far from the prior mean. In this context, the estimates turn out to be again g_0 and accordingly the average minimum cost of error is σ^2 . In the case when the true value of g is g_0 , we find $E[\tilde{g}|g_0] = g_0$.

In the next step, the accuracy with which g can be estimated is characterized by the mean-squared error $E[(\tilde{g} - g)^2|g]$ [23]. The lower bound of the mean-squared error is given by a

quantum Cramér-Rao-type inequality [2]

$$E[(\tilde{g} - g)^2|g] = \text{Tr}\{(\hat{M}_{\min} - g\hat{I})^2\hat{\rho}(g)\} \geq \frac{|x'(g)|}{\text{Tr}\{\hat{\rho}(g)\hat{L}^2\}}, \quad (25)$$

where

$$x'(g) = \text{Tr}\left\{\hat{M}_{\min} \frac{\partial}{\partial g} \hat{\rho}(g)\right\},$$

and the symmetrized logarithmic derivative \hat{L} of the density matrix $\hat{\rho}(g)$ is defined as

$$\frac{\partial \hat{\rho}(g)}{\partial g} = \frac{1}{2}[\hat{L}\hat{\rho}(g) + \hat{\rho}(g)\hat{L}].$$

If we consider the spectral decomposition

$$\hat{\rho}(g) = \cos^2(g\tau_c) e^{-\gamma\tau_f} |e\rangle\langle e| + (1 - \cos^2(g\tau_c) e^{-\gamma\tau_f}) |g\rangle\langle g|,$$

then

$$\hat{L} = -2\tau_c \tan(g\tau_c) |e\rangle\langle e| + \tau_c \frac{\sin(2g\tau_c) e^{-\gamma\tau_f}}{1 - \cos^2(g\tau_c) e^{-\gamma\tau_f}} |g\rangle\langle g|.$$

Hence, we have

$$\begin{aligned} E[(\tilde{g} - g)^2|g] &\geq \frac{1 - \cos^2(g\tau_c) e^{-\gamma\tau_f}}{4\tau_c \sin^2(g\tau_c)} \\ &\quad \times |\sin(2g\tau_c)| \frac{|g_0 - b/a|}{1 - ae^{-\gamma\tau_f}}. \end{aligned} \quad (26)$$

In the inconclusive cases when the experimentalist sets the interaction times either to $\pi/(2g_0)$ or π/g_0 , the inequality in Eq. (26) yields

$$E[(\tilde{g} - g)^2|g] \geq 0,$$

which also means that when we bolster our prior knowledge then the lower bound of the accuracy is the smallest. Now, for the interesting case of $\tau_c = \pi/(4g_0)$, we find

$$\begin{aligned} E[(\tilde{g} - g)^2|g] &\geq \frac{1 - \cos^2\left(\frac{\pi}{4} \frac{g}{g_0}\right) e^{-\gamma\tau_f}}{\sin^2\left(\frac{\pi}{4} \frac{g}{g_0}\right)} \\ &\quad \times \left| \sin\left(\frac{\pi}{2} \frac{g}{g_0}\right) \right| \frac{\sigma^2 e^{-\frac{\pi^2}{8} \frac{\sigma^2}{g_0^2}}}{2 - e^{-\gamma\tau_f}}. \end{aligned}$$

It is worth noting that in the inconclusive situation $\gamma\tau_f \gg 1$, when the estimate of the coupling strength is g_0 , the lower bound of the mean-squared error increases. This fact is in contrast with the inconclusive scenarios where $\tau_c = \pi/(2g_0)$ and $\tau_c = \pi/g_0$, where the left-hand side of the quantum Cramér-Rao inequality is zero, the minimum allowed value. It seems in the context of our system that the extremal behaviors of lower bounds on the accuracy are related only to inconclusive estimation scenarios.

B. Uniform probability density function

In this subsection, we consider a uniform prior PDF. As the only prior knowledge about the coupling g is its mean value g_0 and variance σ^2 , we set the parameter space $\Theta = [g_0 - \sqrt{3}\sigma, g_0 + \sqrt{3}\sigma]$ and PDF

$$z(g) = \frac{1}{2\sqrt{3}\sigma}, \quad g \in \Theta. \quad (27)$$

Like in the previous subsection, we determine the operators defined in Eq. (19)

$$\begin{aligned}\hat{\Gamma}_0 &= \begin{bmatrix} a'e^{-\gamma\tau_f} & 0 \\ 0 & 1 - a'e^{-\gamma\tau_f} \end{bmatrix}, \\ a' &= \frac{1}{2} + \frac{\sin(2\sqrt{3}\sigma\tau_c)\cos(2g_0\tau_c)}{4\sqrt{3}\sigma\tau_c}, \\ \hat{\Gamma}_1 &= \begin{bmatrix} b'e^{-\gamma\tau_f} & 0 \\ 0 & g_0 - b'e^{-\gamma\tau_f} \end{bmatrix}, \\ b' &= \frac{g_0}{2} - \frac{\sin(2g_0\tau_c)\sin(2\sqrt{3}\sigma\tau_c)}{8\sqrt{3}\sigma\tau_c^2} + \frac{\sqrt{3}\sigma\sin(2g_0\tau_c)\cos(2\sqrt{3}\sigma\tau_c) + g_0\cos(2g_0\tau_c)\sin(2\sqrt{3}\sigma\tau_c)}{4\sqrt{3}\sigma\tau_c},\end{aligned}\quad (28)$$

and

$$\begin{aligned}\hat{\Gamma}_2 &= \begin{bmatrix} c'e^{-\gamma\tau_f} & 0 \\ 0 & g_0^2 + \sigma^2 - c'e^{-\gamma\tau_f} \end{bmatrix}, \\ c' &= \frac{g_0^2 + \sigma^2}{2} + \frac{(g_0^2 + 3\sigma^2)\sin(2\sqrt{3}\sigma\tau_c)\cos(2g_0\tau_c)}{4\sqrt{3}\sigma\tau_c} + \frac{\sqrt{3}\sigma\cos(2\sqrt{3}\sigma\tau_c)\cos(2g_0\tau_c) - g_0\sin(2\sqrt{3}\sigma\tau_c)\sin(2g_0\tau_c)}{4\sqrt{3}\sigma\tau_c^2} \\ &\quad - \frac{\sin(2\sqrt{3}\sigma\tau_c)\cos(2g_0\tau_c)}{8\sqrt{3}\sigma\tau_c^3} + \frac{g_0\sin(2g_0\tau_c)\cos(2\sqrt{3}\sigma\tau_c)}{2\tau_c}.\end{aligned}$$

As the structure of the operators $\hat{\Gamma}_k$ ($k = 0, 1, 2$) is the same as in the previous subsection, where we have considered the Gaussian PDF, we obtain for the MMSE estimator

$$\hat{M}_{\min} = \begin{bmatrix} \frac{b'}{a'} & 0 \\ 0 & \frac{g_0 - b'e^{-\gamma\tau_f}}{1 - a'e^{-\gamma\tau_f}} \end{bmatrix}.$$

The average minimum cost of error is

$$\begin{aligned}\bar{C}_{\min} &= g_0^2 + \sigma^2 - \left(\frac{g_0 - b'e^{-\gamma\tau_f}}{1 - a'e^{-\gamma\tau_f}} \right)^2 \\ &\quad - a'e^{-\gamma\tau_f} \left[\frac{b'^2}{a'^2} - \left(\frac{g_0 - b'e^{-\gamma\tau_f}}{1 - a'e^{-\gamma\tau_f}} \right)^2 \right].\end{aligned}$$

The two cases discussed $\tau_c = \pi/(2g_0)$ and $\tau_c = \pi/g_0$ were found to be inconclusive in the previous subsection. It is immediate to see from the structure of $\hat{\Gamma}_k$ that for a uniform prior PDF these cases are not indecisive any more. Thus, supposing that nothing is known in advance about the true value of g in the interval $[g_0 - \sqrt{3}\sigma, g_0 + \sqrt{3}\sigma]$ actually reduces the number of inconclusive scenarios. Let us also reconsider $\tau_c = \pi/(4g_0)$, i.e., the experimentalist expects the TLS to emit a photon with 50% probability, which was seen to be an interesting case of the previous subsection. The MMSE estimator is, in this case,

$$\hat{M}_{\min} = \begin{bmatrix} g_0(1+x) & 0 \\ 0 & g_0\left(1 - \frac{x}{2e^{\gamma\tau_f} - 1}\right) \end{bmatrix},$$

with

$$x = \frac{2}{\pi} \cos\left(\frac{\sqrt{3}\pi\sigma}{2g_0}\right) - \frac{4}{\sqrt{3}\pi^2} \frac{g_0}{\sigma} \sin\left(\frac{\sqrt{3}\pi\sigma}{2g_0}\right).$$

The average minimum cost of error is

$$\bar{C}_{\min} = \sigma^2 - g_0^2 \frac{x^2}{2e^{\gamma\tau_f} - 1}.$$

Measuring the TLS in the excited state results in the estimate

$$\tilde{g} = g_0(1+x),$$

with probability

$$p = \cos^2\left(\frac{\pi}{4} \frac{g}{g_0}\right) e^{-\gamma\tau_f}.$$

Once again we find that when $\gamma\tau_f \gg 1$ this probability reduces to zero and therefore a measurement cannot yield this estimate. Finding the TLS in the ground state results in the estimate

$$\tilde{g} = g_0 \left(1 - \frac{x}{2e^{\gamma\tau_f} - 1} \right),$$

with probability

$$p = 1 - \cos^2\left(\frac{\pi}{4} \frac{g}{g_0}\right) e^{-\gamma\tau_f}.$$

The situation is the same as that for the Gaussian prior PDF; i.e., when $\gamma\tau_f \gg 1$ one measures the TLS to be in the ground state with certainty, the estimate is simply g_0 , and $\bar{C}_{\min} = \sigma^2$. In any case, the average estimator is

$$E[\tilde{g}|g] = g_0 + g_0 x \frac{2\cos^2\left(\frac{\pi}{4} \frac{g}{g_0}\right) - 1}{2e^{\gamma\tau_f} - 1}.$$

We note again the case when the true value of g is g_0 , then $E[\tilde{g}|g_0] = g_0$. If $\gamma\tau_f \gg 1$, then the average estimator is also g_0 no matter what the true value of g is; this is again an inconclusive scenario.

With the uniform prior PDF, the quantum Cramér-Rao inequality is

$$E[(\tilde{g} - g)^2|g] \geq \frac{1 - \cos^2(g\tau_c)e^{-\gamma\tau_f}}{4\tau_c \sin^2(g\tau_c)} \left| \sin(2g\tau_c) \right| \frac{|g_0 - b'/a'|}{1 - a'e^{-\gamma\tau_f}}, \quad (29)$$

which yields, when $\tau_c = \pi/(4g_0)$,

$$E[(\tilde{g} - g)^2 | g] \geq \frac{1 - \cos^2\left(\frac{\pi}{4} \frac{g}{g_0}\right) e^{-\gamma\tau_f}}{\pi \sin^2\left(\frac{\pi}{4} \frac{g}{g_0}\right)} \times \left| \sin\left(\frac{\pi}{2} \frac{g}{g_0}\right) \right| \frac{2g_0^2 |x|}{2 - e^{-\gamma\tau_f}}.$$

The next subsection focuses on numerical simulations in order to understand the role of the detuning Δ and an initial field state with mean photon number larger than zero. We will investigate the deviations from the analytical results of this section and understand the changes inflicted on the estimates, the minimum average cost of error, and the left-hand side of the quantum Cramér-Rao inequality.

C. Numerical results

In the previous subsections, we have calculated analytically the MMSE estimators for both the Gaussian (23) and the uniform (27) PDF. We have presented the simplest scenario, where the cavity field mode is initially in the ground state, $a_0 = 1$, which led to a diagonal form of the density matrix (22). Furthermore, we have considered the single-mode field to be in resonance with the TLS transition, $\Delta = \omega_{e \leftrightarrow g} - \omega_c = 0$, which has allowed us to perform the integrations in Eq. (19). Here, we show the numerical results obtained in more general cases, where the initial state of the field mode is a more general coherent state $|\alpha\rangle$, and where we may have nonzero detuning $\Delta \neq 0$. The coherent state is defined through the parameter α [24],

$$|\alpha\rangle = \sum_{n=0}^{\infty} e^{-\frac{|\alpha|^2}{2}} \frac{\alpha^n}{\sqrt{n!}} |n\rangle, \quad \alpha = |\alpha| e^{i\phi}, \quad (30)$$

where $|n\rangle$ ($n \in \mathbb{N}_0$) are the photon number states and ϕ is the complex phase of α ; the mean photon number of this coherent state is $|\alpha|^2$. Here, we set $\phi = 0$.

Gaussian PDF and resonant interaction $\Delta = 0$. The two parameters of the Gaussian PDF are its mean g_0 and variance σ^2 . To simplify the analysis, we set $\gamma\tau_f = 0$, so that no spontaneous emission may occur. We start our analysis with the simplest case $\alpha = 0$. First of all, we discuss the eigenvalues, i.e., the estimates, of the operator \hat{M}_{\min} . One of the eigenvalues of \hat{M}_{\min} has a discontinuity at $\tau_c = 0$. This can be shown by explicitly taking the limit

$$\lim_{\tau_c \rightarrow 0^+} \frac{g_0 - b}{1 - a} = \frac{g_0(3\sigma^2 + g_0^2)}{\sigma^2 + g_0^2}, \quad (31)$$

with a and b defined in Eq. (24). For $\tau_c = 0$, the function $\frac{g_0 - b}{1 - a}$ is not defined and the eigenvalue can be obtained only by starting again the whole calculation from Eq. (22). The other eigenvalue is continuous and its value tends to g_0 . At $\tau_c = 0$, the eigenvalues of \hat{M}_{\min} are g_0 and 0. This is simply due to the fact that no interaction occurred. Thus, estimates give either the prior expected coupling value or no coupling at all. When τ_c tends to infinity, both curves approach the prior expected value g_0 , and the measurement is again inconclusive. In Fig. 3(a), the average minimum cost of error \bar{C}_{\min} is plotted. At $\tau_c = 0$, we find $\bar{C}_{\min} = \sigma^2$, equal to the prior variance. The plot shows that there is global minimum of \bar{C}_{\min} , which

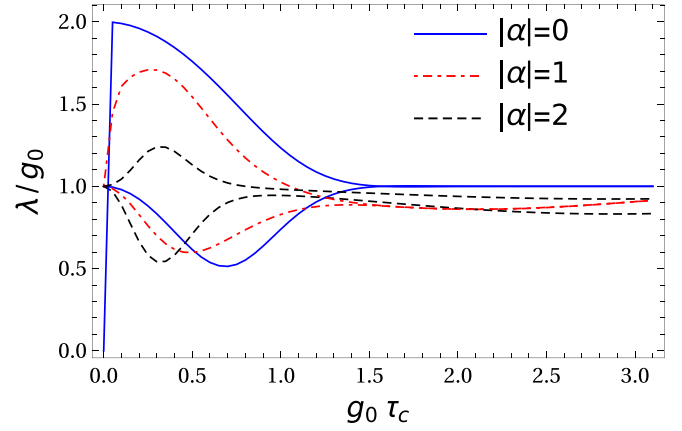


FIG. 2. The eigenvalues of \hat{M}_{\min}/g_0 as a function of $g_0\tau_c$ in the case of the Gaussian prior PDF, with mean g_0 and variance $\sigma^2/g_0^2 = 1$. In the case $\alpha = 0$, the two initial eigenvalues are 0 and g_0 . When $|\alpha| > 0$, the eigenvalues are plotted from $\tau_c = 0^+$, at which time they are equal to g_0 . For large values of τ_c , the eigenvalues tend to the same value g_0 . We set $\gamma\tau_f = 0$, such that no spontaneous decay occurs.

defines the recommended value of $g_0\tau_c$ for the experimental detection. For a fixed value of g_0 , we denote the recommended interaction time as τ_c^* .

Finally, let us discuss the scenarios with finite field amplitude $|\alpha|$, i.e., the initial average photon number becomes nonzero. Now, we have to focus completely on numerical solutions, because analytical calculations are not possible. The numerical results in Fig. 2 show the eigenvalues of \hat{M}_{\min} . Contrary to the behavior encountered for $\alpha = 0$, here all eigenvalues seem to start from g_0 . However, this is true only for $\tau_c = 0^+$. When $\tau_c = 0$, the eigenvalues are 0 and g_0 , but we cannot obtain them because of the finite numerical sum of the field amplitude. Starting from $\tau_c = 0^+$, the eigenvalues are robust against the increase of the terms in the summation provided that the numerical normalization of the coherent state is larger than 0.99. As in the case $\alpha = 0$, the eigenvalues are approaching g_0 as $\tau_c \rightarrow \infty$. The average minimum cost error \bar{C}_{\min} starts for all the values of $|\alpha|$ at $\bar{C}_{\min} = \sigma^2$ and reaches a global minimum for $\tau_c = \tau_c^*$. This value depends on $|\alpha|$ and decreases with increasing $|\alpha|$. As more photons are involved in the interaction, i.e., as the TLS and the field mode undergo many exchanges of photons, more information gets lost in the different photon number states $|n\rangle$. Therefore, the lowest average minimum cost of error is obtained when the field is in the vacuum state, $|\alpha\rangle = |0\rangle$. However, more photons in the interaction result in the appearance of higher Rabi frequencies $g\sqrt{n}$, which in turn means that the minimum value is reached more quickly. We note that different α with the same absolute value show the same behavior both for the eigenvalues of \hat{M}_{\min} and \bar{C}_{\min} , and thus the mean photon number is the only significant variable for the estimation of the dipole coupling strength.

Next, we calculate the average estimator $E[\tilde{g}|g]$, which is determined from the measurement data and from which the value of g can be deduced. Repeated measurements of \hat{M}_{\min} at $\tau_c = \tau_c^*$ give different outcomes whose average is related with the true value g . Figure 3(b) shows some curves for

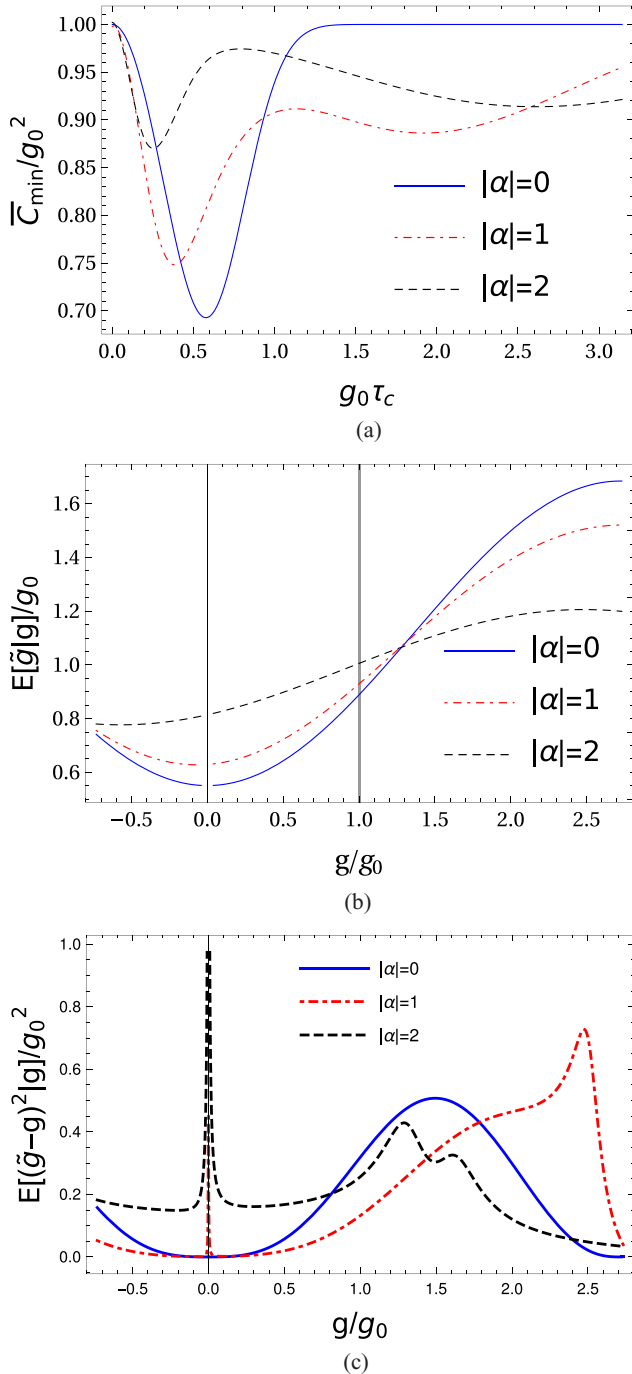


FIG. 3. Figures obtained for a Gaussian prior PDF, with mean g_0 and variance $\sigma^2/g_0^2 = 1$. We set $\gamma\tau_f = 0$, such that no spontaneous decay occurs. In panel (a), each curve has a global minimum that decreases and shifts to larger values of $g_0\tau_c$ with increasing $|\alpha|$. At the time, when \bar{C} attains its minimum, panel (b) displays biased average estimators, where the mean value g_0 of the prior PDF is depicted by a vertical line. The curves in panel (c) characterizing the accuracy of the estimation scenario have to be considered together with the appropriate curves in panel (b) in order to obtain a more complete information about the optimal MMSE estimator. (a) The average minimum cost of error \bar{C}_{\min}/g_0^2 as a function of $g_0\tau_c$. (b) The average estimator $E[\tilde{g}|g]/g_0$ as a function of g/g_0 . (c) The lower bound of the mean-squared error as a function of g/g_0 .

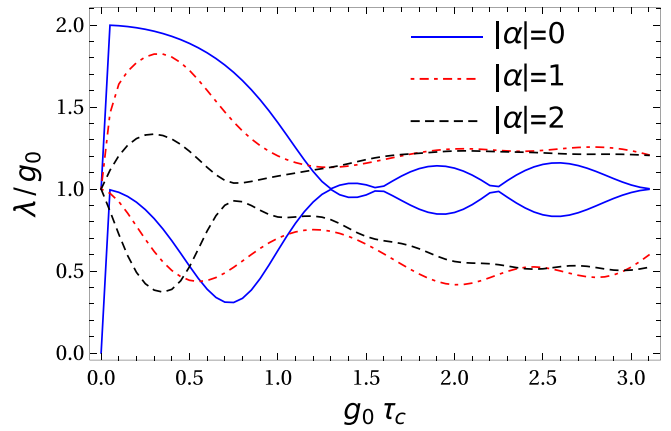


FIG. 4. The eigenvalues of \hat{M}_{\min}/g_0 as a function of $g_0\tau_c$ in the case of the uniform prior PDF with mean g_0 and variance $\sigma^2/g_0^2 = 1$. In the case $\alpha = 0$, the two initial eigenvalues are 0 and g_0 . The eigenvalues are plotted from $\tau_c = 0^+$ for all $|\alpha| > 0$ and their starting values are g_0 . For large values of $g_0\tau_c$, the eigenvalues tend to the same value g_0 , but slower than in Fig. 2. We set $\gamma\tau_f = 0$.

different values of α which clearly demonstrate that the obtained MMSE estimator is biased. Furthermore, using Eq. (25), we plot in Fig. 3(c) the lower bounds of the mean-squared error. In the case $g = g_0$, the lower bound of the mean-squared error decreases whenever $|\alpha| \neq 0$. By taking into account the behavior of the average estimate $E[\tilde{g}|g]$, which at $g = g_0$ approaches the value of g_0 with increasing $|\alpha|$ [see Fig. 3(b)], we can conclude that increasing values of $|\alpha|$ lead to measurement strategies, which reinforce our prior expectations.

Uniform prior PDF and resonant interaction $\Delta = 0$. The two parameters of the uniform PDF are again the mean g_0 and the variance σ^2 . We assume again that no spontaneous emission occurs, i.e., $\gamma\tau_f = 0$. In Fig. 4, the measurement estimates, or the eigenvalues of the MMSE operator \hat{M}_{\min} , are shown. If $\alpha = 0$, the eigenvalues show a discontinuity around at $\tau_c = 0$, as in the case of Gaussian PDF, which can be seen from the analytical calculation of \hat{M}_{\min} . The corresponding limit reads

$$\lim_{\tau_c \rightarrow 0^+} \frac{g_0 - b'}{1 - a'} = \frac{g_0(3\sigma^2 + g_0^2)}{\sigma^2 + g_0^2}, \quad (32)$$

with a' and b' defined in (28). The average cost function \bar{C}_{\min} plotted in Fig. 5(a) starts from the prior variance σ^2 and after reaching a global minimum approaches again the prior variance as $\tau_c \rightarrow \infty$. Figure 5(b) shows the average estimator $E[\tilde{g}|g]$ at the time τ_c^* when \bar{C}_{\min} attains its minimum. The lower bound of the mean-squared error is shown in Fig. 5(c). The behavior of all these curves resembles the Gaussian PDF case, which has already been discussed.

If we set a finite amplitude $|\alpha| > 0$ for the optical field, the eigenvalues of \hat{M}_{\min} are continuous. They both start from the prior mean value g_0 at $\tau_c = 0^+$ and show large oscillations in time. In Fig. 5(a), it is seen that \bar{C}_{\min} always starts from the prior variance σ^2 and reaches a minimum that depends on $|\alpha|$. As in the Gaussian prior PDF case, the absolute value of α is sufficient to characterize completely these minima.

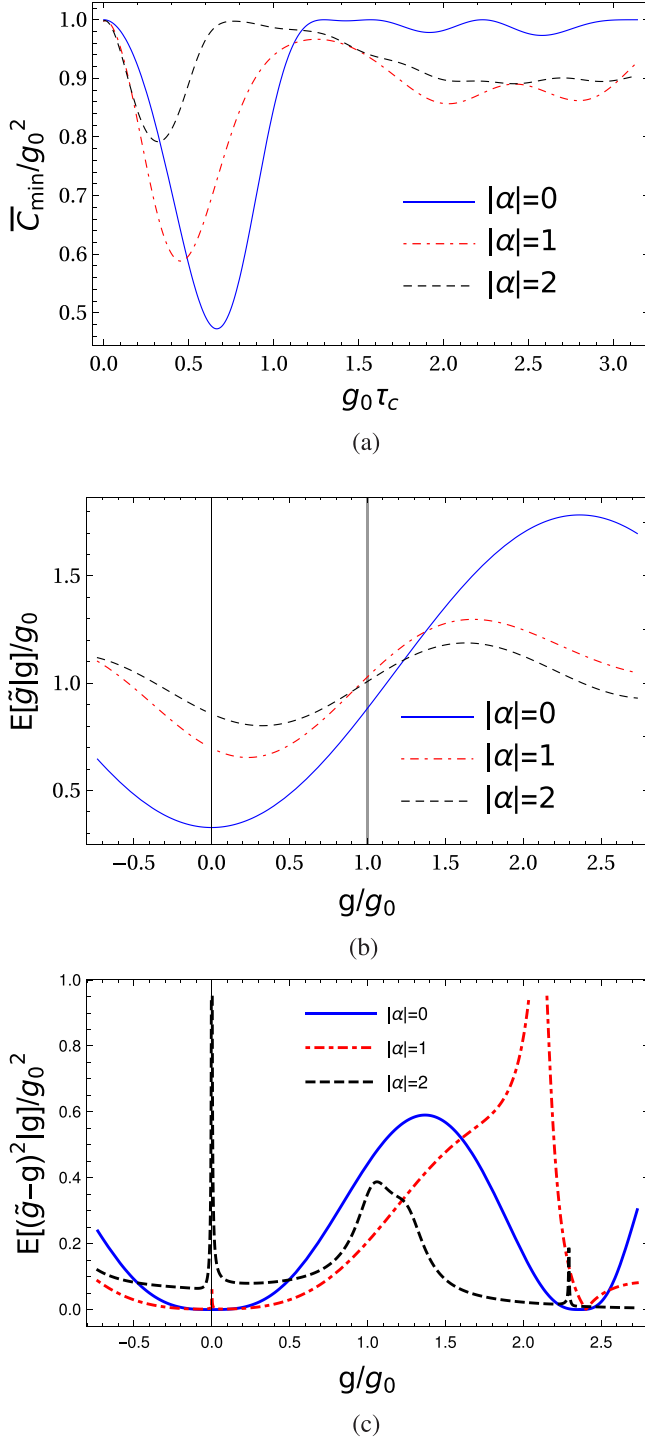


FIG. 5. Figures obtained for a uniform prior PDF. The parameters are set to the same value as in Fig. 3. The curves display very similar properties to those corresponding in Fig. 3. (a) The average minimum cost of error \bar{C}_{\min}/g_0^2 as a function of $g_0\tau_c$. (b) The average estimator $E[\hat{g}|g]/g_0$ as a function of g/g_0 . (c) The lower bound of the mean-squared error as a function of g/g_0 .

Role of the detuning Δ and the flight time τ_f . In order to demonstrate the properties of nonzero detuning in a simple way, we have considered set $\alpha = 0$, $\gamma\tau_f = 0$, and $\tau_c = \tau_c^*$, where the average minimum cost of error reaches

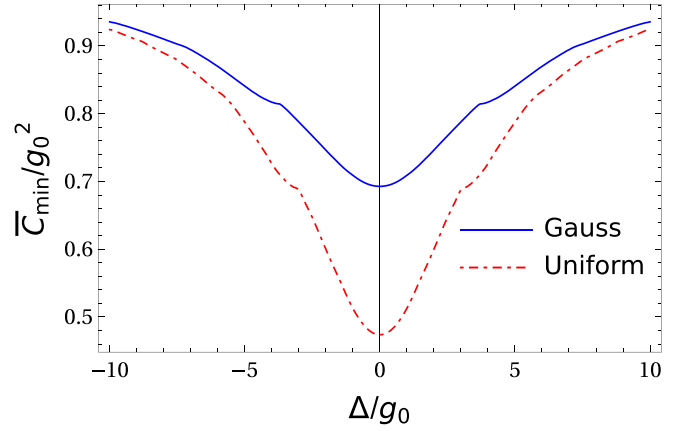


FIG. 6. The average minimum cost of error \bar{C}_{\min}/g_0^2 reached at $\tau_c = \tau_c^*$ as a function of the detuning Δ . The lowest average minimum cost of error is at resonance $\Delta = 0$. We set $\gamma\tau_f = 0$, $\alpha = 0$, and $\sigma^2/g_0^2 = 1$.

its minimum. Figure 6 shows that the minimum of the average minimum cost of error occurs at $\Delta = 0$, for both the Gaussian and the uniform prior PDF. Nonzero detuning decreases the probability of the transition occurring in the TLS and increases the average cost of error. Another interesting feature of the off-resonant case is that for $g_0\tau_c \rightarrow \infty$, \bar{C}_{\min} does not approach σ^2 as in Figs. 3(a) and 5(a), but has a value depending on both Δ and the prior variance σ^2 .

The influence of the flight time τ_f on the estimation scenario is clearly destructive, as we have shown in the previous subsections. Therefore, it is interesting to compare these deleterious effects on the two different prior PDF considered in this work. As a result of our previous findings, we have set $\Delta = 0$, initial single-mode field in the ground state, i.e., $\alpha = 0$, and $\tau_c = \tau_c^*$. Figure 7 shows that the average minimum cost of error at τ_c^* reaches its minimum for $\gamma\tau_f = 0$ and approaches its maximum σ^2 when $\gamma\tau_f \rightarrow \infty$.

In summary, we have been able to identify the most ideal scenario for the implementation of a MMSE estimator. Nonzero detuning, the occurrence of the spontaneous

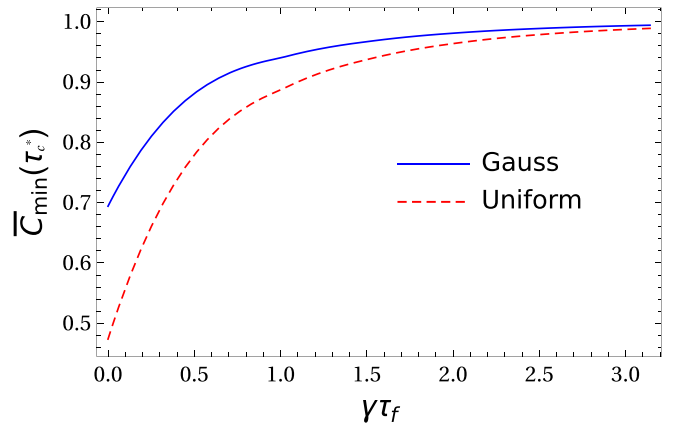


FIG. 7. The average minimum cost of error \bar{C}_{\min}/g_0^2 reached at $\tau_c = \tau_c^*$ as a function of $\gamma\tau_f$. The minimum is reached when $\gamma\tau_f = 0$ and approaches its limit value $\sigma^2/g_0^2 = 1$ with increasing $\gamma\tau_f$. We set $\Delta = 0$ and $\alpha = 0$.

emission and initial states of the field with nonzero mean photon number, should be avoided. If this situation is approximately achievable in some experimental setup, then the interaction time τ_c has to be fixed to values between $0.6/g_0$ and $0.7/g_0$, which is before the appearance of the so-called collapse phenomena in the population inversion of the TLS [9].

D. Comparison with experiments

In this section, we analyze the physical boundaries of our model proposed in Sec. II. Here, we consider a more realistic scenario, where inside the cavity the spontaneous decay γ of the TLS and the damping rate κ of the single-mode field are present. In order to see the boundaries of our model, we take two experimental works: One in the strong coupling regime [25] and the other one in the intermediate coupling regime [26]. In these experimental works, the cavity mode experiences no gains from the outer world, i.e., the mean number of thermal photons is very low, and therefore the evolution can be effectively described by a Markovian master equation

$$\begin{aligned} \dot{\hat{\rho}} = & -i[\hat{H}, \hat{\rho}] + \kappa(\hat{a}\hat{\rho}\hat{a}^\dagger - \frac{1}{2}\{\hat{a}^\dagger\hat{a}, \hat{\rho}\}) \\ & + \gamma(\hat{\sigma}_-\hat{\rho}\hat{\sigma}_+ - \frac{1}{2}\{\hat{\sigma}_+\hat{\sigma}_-, \hat{\rho}\}), \end{aligned} \quad (33)$$

where the Hamiltonian \hat{H} is given in Sec. II and $\{.,.\}$ is the anticommutator. For the sake of simplicity, we consider the detuning $\Delta = 0$ and a pure initial state $|e\rangle|0\rangle$, i.e., the TLS is in the excited state and the cavity in the ground state. The state of the TLS system upon leaving the cavity is obtained from (33) and yields

$$\hat{\rho}(t) = \begin{bmatrix} f(t) & 0 \\ 0 & 1 - f(t) \end{bmatrix}, \quad (34)$$

where

$$\begin{aligned} f(t) = & e^{-(\gamma+\kappa)t/2} \left[-8g^2 \frac{1 + \cosh(\Omega t/2)}{\Omega^2} \right. \\ & \left. + \frac{(\gamma - \kappa)^2 \cosh(\Omega t/2)}{\Omega^2} + \frac{(\kappa - \gamma) \sinh(\Omega t/2)}{\Omega} \right], \end{aligned}$$

with $\Omega = \sqrt{(\gamma - \kappa)^2 - 16g^2}$.

Starting from the density matrix (34), we can apply the formalism of the MMSE estimator to find the average minimum cost of error in (21). According to the Bayesian formulation of the estimation problem with a quadratic cost function, those strategies and situations are more advantageous where the average cost of error is the smallest. Therefore, here we only analyze the average minimum cost of error with values of γ and κ taken from the experimental papers [25] and [26] and compare them with our ideal model in Sec. II for both a Gaussian and a uniform prior PDF, respectively.

Figure 8 shows that the average minimum cost of error is very close to the ideal model in the strong coupling regime, whereas in the intermediate coupling regime the decoherence effects increase \bar{C}_{\min} for almost all interaction times, which means that the optimal estimation strategy is less informative than the ideal one. Similarly to our previous findings, the uniform prior PDF is more suitable than the Gaussian and this

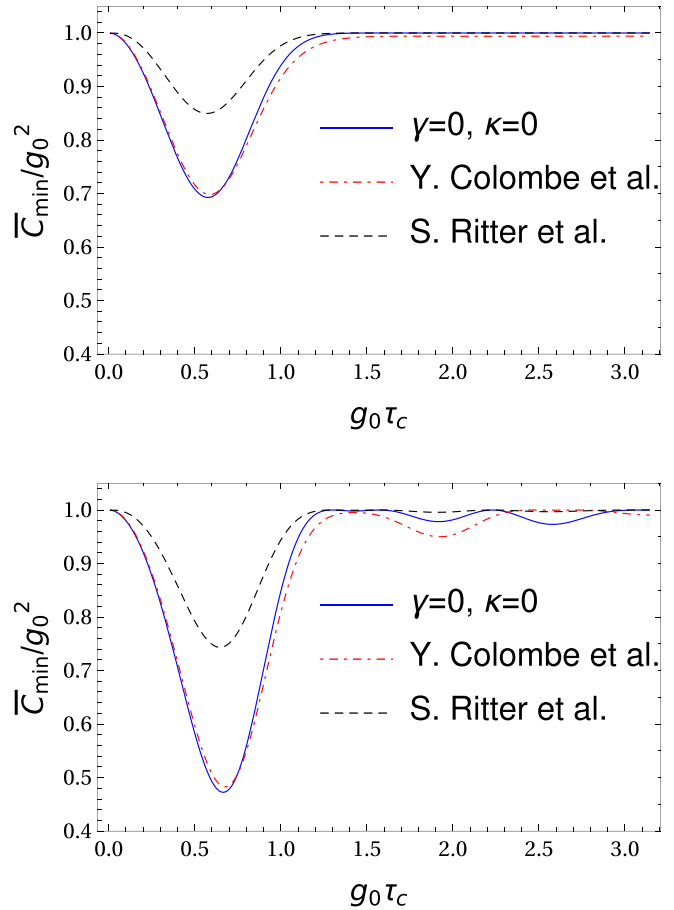


FIG. 8. The average minimum cost of error \bar{C}_{\min}/g_0^2 as a function of $g_0\tau_c$. The blue (solid) line represents the ideal case: $\gamma = \kappa = 0$. The two experimental curves refer to the strong coupling regime ($\gamma/g_0 = 0.014$, $\kappa/g_0 = 0.246$) of Colombe *et al.* [25] and to the intermediate coupling regime ($\gamma/g_0 = 0.6$, $\kappa/g_0 = 0.6$) of Ritter *et al.* [26]. Top: Gaussian prior PDF with mean g_0 and variance $\sigma^2/g_0^2 = 1$. Bottom: Uniform prior PDF with mean g_0 and variance $\sigma^2/g_0^2 = 1$. We set $\gamma\tau_f = 0$, such that no spontaneous decay occurs during the time when the TLS system reaches the detectors.

fact is not influenced by the addition of the decaying mechanisms inside the cavity. In summary, we have considered one of the simplest and demonstrative scenarios, where realistic effects in experimental situations can be compared with our model. Destructive effects of decoherence sources make the estimation strategies less effective, as is expected, and show that our conclusions apply only to strong coupling regimes. In the context of the MMSE estimator, this connection with the experimental parameters is more straightforward to realize because of the more simple formalism than the one used for the ML estimators in the subsequent section. Therefore, we devote the next section only to the model of Sec. II.

V. MAXIMUM-LIKELIHOOD ESTIMATOR

In this section, we are going to determine the ML estimator. The variational problem for the average cost in Eq. (13) reads

$$\bar{C}[\hat{\Pi}] = \text{Tr} \left\{ \int_{\Theta} d\hat{\Pi}(\tilde{g}) z(\tilde{g}) \hat{\rho}(\tilde{g}) \right\}, \quad (35)$$

where we are looking for those infinitesimal operators $d\hat{\Pi}(\tilde{g})$ for which \bar{C} is maximum [due to the negative sign involved in the cost function Eq. (15)]. In order to gain insight, we employ the density matrix in Eq. (22),

$$\hat{\rho}(g) = \begin{bmatrix} \cos^2(g\tau_c)e^{-\gamma\tau_f} & 0 \\ 0 & 1 - \cos^2(g\tau_c)e^{-\gamma\tau_f} \end{bmatrix},$$

where the detuning $\Delta = 0$ and the initial state of the field is in the ground state. Integrals of $d\hat{\Pi}(\tilde{g})$ on compact intervals result in elements of the POVM, and thus the following construction,

$$d\hat{\Pi}(\tilde{g}) = \begin{bmatrix} f_I(\tilde{g}) + f_z(\tilde{g}) & f_x(\tilde{g}) - if_y(\tilde{g}) \\ f_x(\tilde{g}) + if_y(\tilde{g}) & f_I\tilde{g} - f_z(\tilde{g}) \end{bmatrix} d\tilde{g}, \quad (36)$$

with $f_I, f_z, f_y,$ and f_x being real functions, ensures the self-adjointness of the infinitesimal generator. We are going to employ this ansatz and solve the variational problem in Eq. (35). Only after this step are we going to impose the constraints of the POVM in Eq. (10). In the following, we reconsider the two cases of the PDF $z(g)$ used in Sec. IV.

A. Gaussian probability density function

We assume again that g is characterized by its mean value g_0 and variance σ^2 . The prior PDF is set to be Eq. (23) with $\Theta = \mathbb{R}$. Then the average cost function reads

$$\bar{C} = \frac{1}{\sqrt{2\pi\sigma^2}} \int_{\mathbb{R}} e^{-\frac{(g-g_0)^2}{2\sigma^2}} [f_I(\tilde{g}) - f_z(\tilde{g})(1 - e^{-\gamma\tau_f}) + f_z(\tilde{g}) \cos(2\tilde{g}\tau_c)e^{-\gamma\tau_f}] d\tilde{g}. \quad (37)$$

$$f_I(\sigma x + g_0) = \sum_{n=0}^{\infty} \gamma_n^I \Psi_n(x), \quad f_z(\sigma x + g_0) = \sum_{n=0}^{\infty} \gamma_n^z \Psi_n(x), \quad \text{and} \quad \cos(2\sigma x\tau_c + 2g_0\tau_c)e^{-x^2/2} = \sum_{n=0}^{\infty} \gamma_n^c \Psi_n(x),$$

and, with the help of an integral formula involving Hermite polynomials [28,29], we have

$$\gamma_n^c = \langle \cos(2\sigma x\tau_c + 2g_0\tau_c)e^{-x^2/2}, \Psi_n(x) \rangle = \frac{\pi^{1/4}}{\sqrt{2^n n!}} \begin{cases} (-1)^{n/2} (2\sigma\tau_c)^n e^{-\sigma^2\tau_c^2} \cos(2g_0\tau_c) & n \text{ is even,} \\ (-1)^{(n+1)/2} (2\sigma\tau_c)^n e^{-\sigma^2\tau_c^2} \sin(2g_0\tau_c) & n \text{ is odd.} \end{cases} \quad (40)$$

Now, upon substituting these expansions into Eq. (38) and taking into account the properties of the orthonormal basis, we obtain

$$\bar{C} = \frac{1}{\sqrt{2\sqrt{\pi}}} \left[\gamma_0^I - \gamma_0^z (1 - e^{-\gamma\tau_f}) + \frac{e^{-\gamma\tau_f}}{\pi^{1/4}} \sum_{n=0}^{\infty} \gamma_n^z \gamma_n^c \right], \quad (41)$$

where we have used the relation $e^{-x^2/2}/\pi^{1/4} = \Psi_0(x)$. We observe that \bar{C} depends only on γ_0^I , the first coefficient in the expansion of $f_I(ax + b)$, and therefore we set $\gamma_n^I = 0$ for $n \neq 0$. Thus,

$$f_I(\sigma x + g_0) = \frac{\gamma_0^I}{\pi^{1/4}} e^{-x^2/2},$$

and replacing $\sigma x + g_0$ with x we have

$$f_I(x) = \frac{\gamma_0^I}{\pi^{1/4}} e^{-\frac{(x-g_0)^2}{2\sigma^2}}.$$

We have recast the variational problem to an equivalent one where we search for the real functions f_I and f_z such that \bar{C} in Eq. (37) is maximum. As \bar{C} does not depend on f_x and f_y , we set them to zero. Upon applying the transformation $\tilde{g} \rightarrow \sigma x + g_0$, Eq. (37) becomes

$$\bar{C} = \frac{1}{\sqrt{2\pi}} \int_{\mathbb{R}} dx e^{-x^2/2} [f_z(\sigma x + g_0)(e^{-\gamma\tau_f} - 1) + f_z(\sigma x + g_0) \times \cos(2\sigma x\tau_c + 2g_0\tau_c)e^{-\gamma\tau_f} + f_I(\sigma x + g_0)]. \quad (38)$$

The above variational problem can be solved if we focus on square integrable functions which form the Hilbert space $\mathbb{L}^2(\mathbb{R})$ (see Ref. [27]). We consider now the following functions,

$$\Psi_n(x) = e^{-x^2/2} \frac{H_n(x)}{\sqrt{\pi} 2^n n!}, \quad n = 0, 1, 2, \dots, \quad (39)$$

where $H_n(x)$ is the n th-order Hermite polynomial with the property

$$\int_{\mathbb{R}} H_n(x) H_m(x) e^{-x^2} dx = \sqrt{\pi} 2^n n! \delta_{nm}.$$

Thus, the functions in Eq. (39) form an orthonormal basis in $\mathbb{L}^2(\mathbb{R})$, in which the inner product is given by the integral

$$\langle f, g \rangle = \int_{\mathbb{R}} \overline{f(x)} g(x) dx.$$

In the next step, we make use of the fact that every function in the Hilbert space can be expanded in the orthonormal basis. Hence,

Furthermore, \bar{C} is maximum with respect to $\{\gamma_n^z\}_{n=0}^{\infty}$ whenever $\gamma_n^z = \text{constant} \times \gamma_n^c$ or in other words the functions $\cos(2\sigma x\tau_c + 2g_0\tau_c)e^{-x^2/2}$ and $f_z(\sigma x + g_0)$ are parallel with respect to the inner product $\langle \cdot, \cdot \rangle$. In fact, this means that

$$f_z(x) = c \cos(2\tau_c x) e^{-\frac{(x-g_0)^2}{2\sigma^2}}, \quad c > 0.$$

We recall the following condition on the POVM,

$$\int_{\mathbb{R}} d\hat{\Pi}(x) = \hat{I},$$

which, due to Eq. (36), is equivalent to

$$\int_{\mathbb{R}} f_I(x) dx = 1 \quad \text{and} \\ \int_{\mathbb{R}} f_z(x) dx = \sigma \int_{\mathbb{R}} f_z(\sigma x + g_0) dx = 0.$$

Then $\gamma_0^l = 1/\sqrt{2\sqrt{\pi}\sigma^2}$ and $\gamma_n^z = 0$ for even n , the latter being due to the fact that integration of a symmetric function about the origin over the whole real line is zero and every odd term of the orthonormal basis is such a function. We hence have

$$\int_{\mathbb{R}} \Psi_n(x) dx = 0, \quad n \text{ is odd.}$$

Thus,

$$f_I(x) = \frac{1}{\sqrt{2\pi}\sigma^2} e^{-\frac{(x-g_0)^2}{2\sigma^2}} \text{ and}$$

$$f_z(\sigma x + g_0) = c \times \sum_{n \text{ odd}} \gamma_n^c \Psi_n(x). \quad (42)$$

There is one more requirement, namely that

$$\int_{\Delta} d\hat{\Pi}(x) = \hat{\Pi}(\Delta)$$

is a positive semidefinite operator with a spectrum confined to the interval $[0,1]$ for every compact interval Δ in \mathbb{R} . This equivalent to

$$0 \leq \int_{\Delta} [f_I(x) \pm f_z(x)] dx \leq 1, \quad \forall \Delta \in \mathbb{R}. \quad (43)$$

We consider the compact interval $\Delta = [a, b]$ with arbitrary $a, b \in \mathbb{R}$ and $b > a$. Using the results of Eq. (40), we have

$$\sum_{n \text{ odd}} \gamma_n^c \Psi_n(x) = -\sin(2g_0\tau_c) \sin(2\sigma x\tau_c) e^{-x^2/2}.$$

In view of the above relation,

$$0 \leq \int_a^b e^{-x^2/2} \left[\frac{1}{\sqrt{2\pi}} \pm c\sigma \sin(2g_0\tau_c) \sin(2\sigma x\tau_c) \right] dx \leq 1,$$

where we have again employed the variable transformation $x \rightarrow \sigma x + g_0$ in Eq. (43). In order to analyze the right-hand-side inequality, we first make some observations. The area under the function $e^{-x^2/2}/\sqrt{2\pi}$ around the origin contributes the most due to the properties of the error function $\text{erf}(x)$ [30] and $\sin(2\sigma x\tau_c)e^{-x^2/2}$ is an odd function. Therefore, if the following inequalities

$$0 \leq \int_0^{\frac{\pi}{2\sigma\tau_c}} e^{-x^2/2} \left[\frac{1}{\sqrt{2\pi}} - cy \sin(2\sigma x\tau_c) \right] dx,$$

$$\int_0^{\frac{\pi}{2\sigma\tau_c}} e^{-x^2/2} \left[\frac{1}{\sqrt{2\pi}} + cy \sin(2\sigma x\tau_c) \right] dx \leq 1,$$

$$y = \sigma |\sin(2g_0\tau_c)|,$$

with $\sigma, \tau_c > 0$ and $2g_0\tau_c \neq \pi + k\pi$ ($k \in \mathbb{Z}$) hold, then no matter how we choose our intervals the condition (43) is fulfilled. In the case when $2g_0\tau_c = \pi + k\pi$ ($k \in \mathbb{Z}$),

condition (43) is automatically satisfied. Making use of the error function, we obtain

$$c \leq \frac{2}{\sqrt{2\pi}\sigma^2 |\sin(2g_0\tau_c)| e^{-2\sigma^2\tau_c^2}} \times \frac{\text{erf}\left(\frac{\pi}{2\sqrt{2}\sigma\tau_c}\right)}{\text{erf}\left(\frac{\pi+4i\sigma^2\tau_c^2}{2\sqrt{2}\sigma\tau_c}\right) + \text{erf}\left(\frac{\pi-4i\sigma^2\tau_c^2}{2\sqrt{2}\sigma\tau_c}\right)} = c_1, \text{ and}$$

$$c \leq \frac{2}{\sqrt{2\pi}\sigma^2 |\sin(2g_0\tau_c)| e^{-2\sigma^2\tau_c^2}} \times \frac{2 - \text{erf}\left(\frac{\pi}{2\sqrt{2}\sigma\tau_c}\right)}{\text{erf}\left(\frac{\pi+4i\sigma^2\tau_c^2}{2\sqrt{2}\sigma\tau_c}\right) + \text{erf}\left(\frac{\pi-4i\sigma^2\tau_c^2}{2\sqrt{2}\sigma\tau_c}\right)} = c_2. \quad (44)$$

As our original task was to maximize the average cost function \bar{C} , the relevant functions read

$$f_I(x) = \frac{1}{\sqrt{2\pi}\sigma^2} e^{-\frac{(x-g_0)^2}{2\sigma^2}} \text{ and}$$

$$f_z(x) = -c_{\max} \sin(2g_0\tau_c) \sin[2\tau_c(x - g_0)] e^{-\frac{(x-g_0)^2}{2\sigma^2}},$$

with $c_{\max} = \min\{c_1, c_2\}$. Together with the ansatz (36), we have determined the ML estimators. Finally, the maximum of the average cost function reads

$$\bar{C}_{\max} = \frac{1}{\sqrt{4\pi}\sigma^2} + c_{\max} \frac{e^{-\gamma\tau_f}}{\sqrt{2}} e^{-2\sigma^2\tau_c^2} \sin^2(2g_0\tau_c) \underbrace{\sum_{n \text{ odd}} \frac{(2\sigma^2\tau_c^2)^n}{n!}}_{\sinh(2\sigma^2\tau_c^2)}$$

$$= \frac{1}{\sqrt{4\pi}\sigma^2} + c_{\max} e^{-\gamma\tau_f} \frac{1 - e^{-4\sigma^2\tau_c^2}}{2\sqrt{2}} \sin^2(2g_0\tau_c). \quad (45)$$

The three inconclusive cases identified for the MMSE estimator, i.e., $\gamma\tau_f \gg 1$, $\tau_c = \pi/g_0$, and $\tau_c = \pi/(2g_0)$, reduce the value of \bar{C}_{\max} . It becomes clear that, whichever strategy is adopted, these cases should be avoided. The conditional PDF in Eq. (12), $p(\tilde{g}|g)$, is not an even function of the variable $g - \tilde{g}$, and therefore the ML estimate will be biased.

The average estimator reads

$$E[\tilde{g}|g] = \int_{\mathbb{R}} \tilde{g} p(\tilde{g}|g) d\tilde{g} = g_0 + 4\sqrt{5\pi} c_{\max} \sigma^2 \tau_c \times e^{-2\sigma^2\tau_c^2 - \gamma\tau_f} [e^{\gamma\tau_f} - 2\cos^2(g\tau_c)] \sin(2g_0\tau_c). \quad (46)$$

Here, the quantum Cramér-Rao inequality has the same form as in Eq. (25), i.e.,

$$E[(\tilde{g} - g)^2|g] \geq \frac{|x'(g)|}{\text{Tr}\{\hat{\rho}(g)\hat{L}^2\}} \quad (47)$$

but

$$x'(g) = \int_{-\infty}^{\infty} \tilde{g} \text{Tr} \left\{ \frac{\partial}{\partial g} \hat{\rho}(g) d\hat{\Pi}(\tilde{g}) \right\},$$

and, similarly to Sec. IV,

$$\hat{L} = -2\tau_c \tan(g\tau_c) |e\rangle\langle e| + \tau_c \frac{\sin(2g\tau_c) e^{-\gamma\tau_f}}{1 - \cos^2(g\tau_c) e^{-\gamma\tau_f}} |g\rangle\langle g|.$$

Inserting Eqs. (36) and (45) into Eq. (47), we obtain

$$E[(\tilde{g} - g)^2 | g] \geq \frac{1 - \cos^2(g\tau_c)e^{-\gamma\tau_f}}{\sin^2(g\tau_c)} |\sin(2g\tau_c)| \times 2\sqrt{5\pi}\sigma^2 e^{-2\sigma^2\tau_c^2} |c_{\max} \sin(2g_0\tau_c)|. \quad (48)$$

B. Uniform probability density function

As in the previous subsection, we assume that the coupling strength g has mean value g_0 and variance σ^2 . The prior PDF is set to be Eq. (27) with $\Theta = [g_0 - \sqrt{3}\sigma, g_0 + \sqrt{3}\sigma]$. Now, the average cost function reads

$$\bar{C} = \frac{1}{2\sqrt{3}\sigma} \int_{g_0 - \sqrt{3}\sigma}^{g_0 + \sqrt{3}\sigma} [f_I(\tilde{g}) - f_z(\tilde{g})(1 - e^{-\gamma\tau_f}) + f_z(\tilde{g}) \cos(2\tilde{g}\tau_c)e^{-\gamma\tau_f}] d\tilde{g}. \quad (49)$$

We employ the transformation $\tilde{g} \rightarrow \sqrt{3}\sigma x + g_0$ and obtain

$$\bar{C} = \frac{1}{2} \int_{-1}^1 [f_I(\sqrt{3}\sigma x + g_0) - f_z(\sqrt{3}\sigma x + g_0)(1 - e^{-\gamma\tau_f}) + f_z(\sqrt{3}\sigma x + g_0) \cos(2\sqrt{3}\sigma x\tau_c + 2g_0\tau_c)e^{-\gamma\tau_f}] dx.$$

This time the Hilbert space is $\mathbb{L}^2([-1, 1])$ and we choose the following orthonormal basis [27]:

$$\begin{aligned} \Psi_{n,e}(x) &= \frac{1}{\sqrt{2}} \cos(n\pi x), \\ \Psi_{n,o}(x) &= \frac{1}{\sqrt{2}} \sin(n\pi x), \quad n \in \mathbb{Z}, \end{aligned} \quad (50)$$

where $\Psi_{0,e}(x) = 1/\sqrt{2}$ and $\Psi_{0,o}(x) = 0$. Every function can be expanded in this orthonormal basis. Thus,

$$\begin{aligned} f_I(\sqrt{3}\sigma x + g_0) &= \sum_{i=e,o} \sum_{n=0}^{\infty} \gamma_{n,i}^I \Psi_{n,i}(x), \\ f_z(\sqrt{3}\sigma x + g_0) &= \sum_{i=e,o} \sum_{n=0}^{\infty} \gamma_{n,i}^z \Psi_{n,i}(x), \\ \cos(2\sqrt{3}\sigma x\tau_c + 2g_0\tau_c) &= \sum_{i=e,o} \sum_{n=0}^{\infty} \gamma_{n,i}^c \Psi_{n,i}(x), \end{aligned}$$

and

$$\begin{aligned} \gamma_{n,e}^c &= \langle \cos(2\sqrt{3}\sigma x\tau_c + 2g_0\tau_c), \Psi_{n,e}(x) \rangle \\ &= \frac{4\sqrt{3}\sigma\tau_c \sin(2\sqrt{3}\sigma\tau_c) \cos(2g_0\tau_c)}{\sqrt{2}(12\sigma^2\tau_c^2 - n^2\pi^2)} \cos(n\pi) \quad \text{and} \\ \gamma_{n,o}^c &= \langle \cos(2\sqrt{3}\sigma x\tau_c + 2g_0\tau_c), \Psi_{n,o}(x) \rangle \\ &= -\frac{n\pi \sin(2\sqrt{3}\sigma\tau_c) \sin(2g_0\tau_c)}{\sqrt{2}(12\sigma^2\tau_c^2 - n^2\pi^2)} \cos(n\pi). \end{aligned} \quad (51)$$

Now, taking into account the properties of this orthonormal basis, we obtain

$$\bar{C} = \frac{1}{2} \left[\gamma_0^I - \gamma_0^z(1 - e^{-\gamma\tau_f}) + e^{-\gamma\tau_f} \sum_{i=e,o} \sum_{n=0}^{\infty} \gamma_{n,i}^z \gamma_{n,i}^c \right],$$

a very similar expression to Eq. (41). We observe again that \bar{C} depends only on γ_0^I and therefore we set $\gamma_n^I = 0$ for $n \neq 0$. The condition on the POVM

$$\int_{g_0 - \sqrt{3}\sigma}^{g_0 + \sqrt{3}\sigma} d\hat{\Pi}(x) = \hat{I}$$

results in

$$\int_{g_0 - \sqrt{3}\sigma}^{g_0 + \sqrt{3}\sigma} f_I(x) dx = \int_{g_0 - \sqrt{3}\sigma}^{g_0 + \sqrt{3}\sigma} \frac{\gamma_0^I}{\sqrt{2}} dx = 1$$

and thus $\gamma_0^I = 1/(\sqrt{6}\sigma)$. Similar to the previous subsection, we have

$$\int_{g_0 - \sqrt{3}\sigma}^{g_0 + \sqrt{3}\sigma} f_z(x) dx = \sqrt{3}\sigma \int_{-1}^1 f_z(\sqrt{3}\sigma x + g_0) dx = 0,$$

which yields $\gamma_{0,e}^z = 0$. As we would like to maximize \bar{C} , we set $\gamma_{n,i}^z = \text{constant} \times \gamma_{n,i}^c$ for $n \neq 0$ ($i \in \{e, o\}$), a similar geometrical strategy to the one employed in the previous subsection. Thus,

$$\begin{aligned} f_I(x) &= \frac{1}{2\sqrt{3}\sigma} \quad \text{and} \\ f_z(x) &= c \left[\cos(2x\tau_c) - \frac{\sin(2\sqrt{3}\sigma\tau_c) \cos(2g_0\tau_c)}{2\sqrt{3}\sigma\tau_c} \right], \end{aligned} \quad (52)$$

with $c > 0$. Imposing the constraint that

$$\int_{\Delta} d\hat{\Pi}(x) = \hat{\Pi}(\Delta)$$

is a positive semidefinite operator with a spectrum confined to the interval $[0, 1]$ for every compact interval Δ in $[g_0 - \sqrt{3}\sigma, g_0 + \sqrt{3}\sigma]$, we find

$$0 \leq \int_a^b [f_I(x) \pm f_z(x)] dx \leq 1, \quad (53)$$

where $b \leq g_0 + \sqrt{3}\sigma$ and $a \geq g_0 - \sqrt{3}\sigma$. After performing the definite integral, we get

$$\begin{aligned} 0 \leq x \pm \frac{c}{\tau_c} [\sin(x2\sqrt{3}\sigma\tau_c) \cos(y2g_0\tau_c) \\ - x \sin(2\sqrt{3}\sigma\tau_c) \cos(2g_0\tau_c)] \leq 1, \quad x = \frac{b-a}{2\sqrt{3}\sigma} \in [0, 1], \\ y = \frac{b+a}{2g_0} \in [1 - \sqrt{3}\sigma(1-x)/g_0, 1 + \sqrt{3}\sigma(1-x)/g_0], \end{aligned} \quad (54)$$

with $g_0 \neq 0$. It is interesting to note the extreme cases $x = 0$ and $x = 1$, when the term

$$\begin{aligned} f_{\pm}(x, y, c) &= x \pm \frac{c}{\tau_c} [\sin(x2\sqrt{3}\sigma\tau_c) \cos(y2g_0\tau_c) \\ &\quad - x \sin(2\sqrt{3}\sigma\tau_c) \cos(2g_0\tau_c)] \end{aligned} \quad (55)$$

is equal to 0 and 1, respectively. The functions $f_+(x, y, c)$ and $f_-(x, y, c)$ are continuous in x and have extrema, where they can violate the conditions of being smaller than 1 and greater than 0. The strategy is to find these points $x_{\text{ext}} = x_{\text{ext}}(c)$. Upon replacing these back to into Eq. (54), one is able to find

c_{\max} . In order to demonstrate the procedure, let us consider $2\sqrt{3}\sigma\tau_c = 2g_0\tau_c = \pi/2$. Then, Eq. (55) reads

$$f_{\pm}(x, y, c) = x \pm \frac{c}{\tau_c} \sin\left(x\frac{\pi}{2}\right) \cos\left(y\frac{\pi}{2}\right),$$

$$x \in [0, 1], \quad y \in [x, 2-x].$$

The two extrema of $f_{\pm}(x, y, c)$ are found at $y = x$ (minimum) and $y = 2 - x$ (maximum), yielding

$$1 - \frac{c\pi}{2\tau_c} \cos(x_{\min}^- \pi) = 0,$$

$$1 + \frac{c\pi}{2\tau_c} \cos(x_{\max}^- \pi) = 0.$$

These equations, together with Eq. (54), result in

$$c \leq \frac{2\tau_c}{\pi} = c_1.$$

$f_+(x, y, c)$ has two extrema at $y = x$ (maximum) and $y = 2 - x$ (minimum), and therefore we have

$$c \leq \frac{2\tau_c}{\pi} = c_2 = c_1.$$

Finally, the task to maximize \bar{C} yields

$$c_{\max} = \min\{c_1, c_2\} = c_1. \quad (56)$$

The functions defining the ML estimator through the ansatz (36) finally read

$$f_l(x) = \frac{1}{2\sqrt{3}\sigma} \text{ and}$$

$$f_z(x) = c_{\max} \left[\cos(2x\tau_c) - \frac{\sin(2\sqrt{3}\sigma\tau_c) \cos(2g_0\tau_c)}{2\sqrt{3}\sigma\tau_c} \right].$$

The maximum of the average cost function is

$$\bar{C}_{\max} = \frac{1}{2\sqrt{3}\sigma} + c_{\max} \left[\frac{1}{2} - \frac{\sin^2(2\sqrt{3}\sigma\tau_c) \cos^2(2g_0\tau_c)}{12\sigma^2\tau_c^2} + \frac{\sin(4\sqrt{3}\sigma\tau_c) \cos(4g_0\tau_c)}{8\sqrt{3}\sigma\tau_c} \right] e^{-\gamma\tau_f}. \quad (57)$$

The conditional PDF $p(\tilde{g}|g)$ in Eq. (12) is again not an even function of the variable $g - \tilde{g}$. Therefore, the ML estimate, as in the case of the prior Gaussian PDF, will be biased.

In the special case $2\sqrt{3}\sigma\tau_c = 2g_0\tau_c = \pi/2$ discussed earlier,

$$\bar{C}_{\max} = \frac{1}{4g_0} (2 + e^{-\gamma\tau_f}),$$

and the average estimator reads

$$E[\tilde{g}|g] = \int_0^{\frac{\pi}{2\tau_c}} \tilde{g} p(\tilde{g}|g) d\tilde{g}$$

$$= g_0 + \frac{4g_0}{\pi^2} \left[1 - 2e^{-\gamma\tau_f} \cos^2\left(\frac{g}{g_0} \frac{\pi}{4}\right) \right].$$

Furthermore, the inequality for the mean-squared error in Eq. (48) yields

$$E[(\tilde{g} - g)^2|g] \geq \frac{8g_0^2}{\pi^2} \frac{1 - \cos^2\left(\frac{\pi}{4} \frac{g}{g_0}\right) e^{-\gamma\tau_f}}{\pi \sin^2\left(\frac{\pi}{4} \frac{g}{g_0}\right)} \left| \sin\left(\frac{\pi}{2} \frac{g}{g_0}\right) \right|.$$

C. Numerical results

In the previous subsections, we have calculated analytically the ML estimators for both the Gaussian (23) and the uniform (27) prior PDF. Because of the analytically involved solutions, we have used the density matrix in Eq. (22), where $\Delta = 0$ and the field mode is initially in the vacuum state. Therefore, the only parameters left for the numerical investigations are the spontaneous decay rate $\gamma\tau_f$ and the interaction time τ_c . We have shown in the case of the uniform prior PDF that in Eq. (57) the calculation of c_{\max} is very intricate and very much depends on the relation between the variance σ^2 and the mean g_0 . Therefore, we consider here only the ML estimator obtained for the Gaussian prior PDF.

Figure 9(a) shows the numerical evaluation of the average maximum cost function \bar{C}_{\max} . It shows that the best time to perform the measurements is approximately $g_0\tau_c = \frac{\pi}{4} + k\pi$, cf. Eq. (45), with $k \in \mathbb{N}_0$ and with better results as k increases. This means that as the interaction between the field and the TLS is longer, the average cost becomes bigger. The spontaneous decay rate $\gamma\tau_f$ affects the quality of the estimation by reducing \bar{C}_{\max} . However, on the other hand, Fig. 9(b) shows that the average estimate conditioned on the mean g_0 , a possible true value of g , for long interaction times is simply equal to our prior expectation. This type of dichotomy has been found by us [6], where a more optimal average cost function merely leads to the reinforcement of our prior knowledge. Finally, the lower bound of the mean-squared error in Fig. 9(c) demonstrates the decrease of the accuracy of the estimation caused by the increase of $\gamma\tau_f$.

VI. CONCLUSIONS

We have discussed Bayesian-inference approaches with a special focus on the dipole coupling of matter-field interactions. Our scheme is based on two-level systems (TLSs) which transit through a cavity and interact with a single-mode radiation field. The state of the TLS is subsequently measured. Spontaneous emission of the excited state of the TLS is taken into account. Our protocol assumes that all the TLSs are prepared initially in the excited states, and that the cavity field is reset before the transit of each TLS. We have derived the minimum mean-square error (MMSE) estimator for both the Gaussian and the uniform probability density functions (PDF) with given mean and variance. It has been demonstrated that the detuning between the TLS transition frequency and the cavity resonance frequency has a destructive effect on parameter estimation. Furthermore, spontaneous emission, as well as interaction times that are too long or too short, result in the reinforcement of our prior expectations. In the case of resonant interactions with initial ground state of the field mode, we have explicitly shown that the MMSE estimator \hat{M}_{\min} is diagonal in the basis of the qubit. Dividing \hat{M}_{\min} in Eq. (24) by the prior mean g_0 results in a positive-operator valued measurement (POVM) element associated with an inefficient measurement scenario,

$$\hat{\Pi} = \eta_1 |e\rangle\langle e| + \eta_2 |g\rangle\langle g|, \quad 0 \leq \eta_1, \eta_2 \leq 1,$$

where the detection efficiencies are characterized by η_1 and η_2 . These efficiencies are known functions of the prior expected parameter values according to Eq. (24). For example,

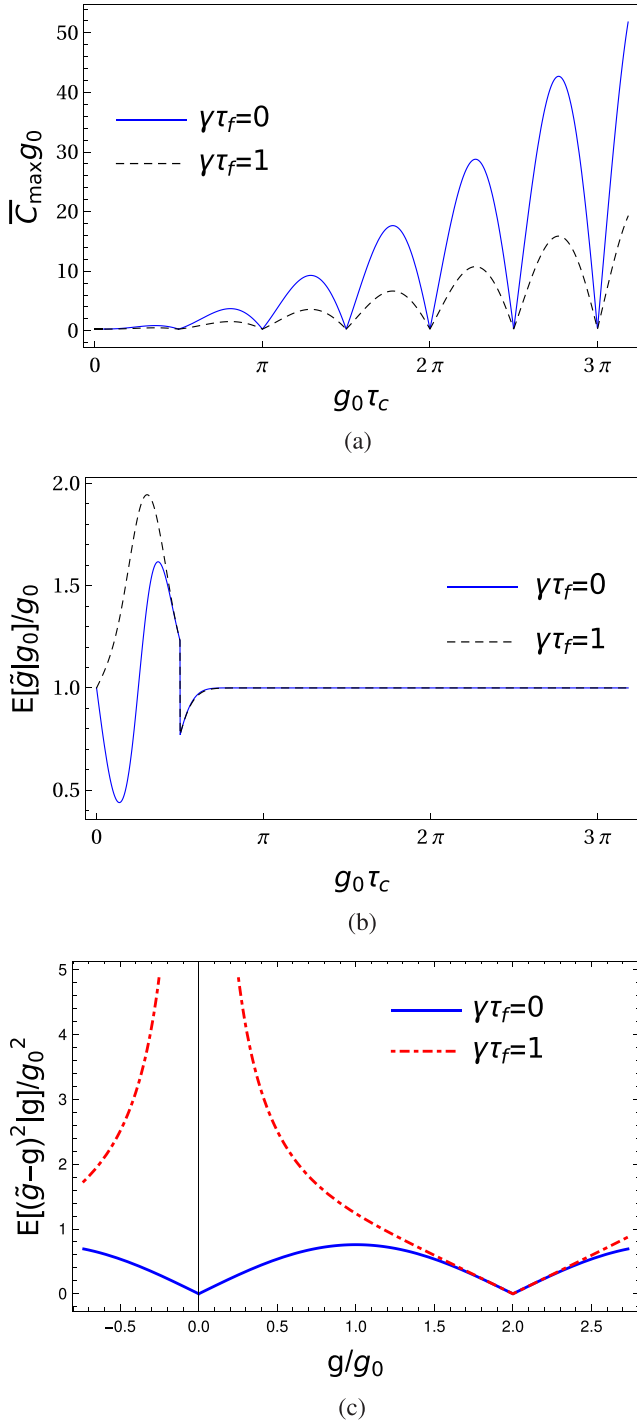


FIG. 9. Figures obtained in the case of the Gaussian prior PDF. We set $\sigma^2/g_0^2 = 1$. We see that spontaneous decay reduces the average cost function (a). In panel (b), we set $g = g_0$. We see there is a jump at $g_0\tau_c = \pi/2$ due to the properties of c_{\max} defined in Eqs. (44) and (45). In panel (c), the interaction time is $\tau_c = \pi/(4g_0)$. (a) The average maximum cost function $\bar{C}_{\max}g_0$ as a function of $g_0\tau_c$. (b) The average estimator $E[|\tilde{g}|g_0]/g_0$ as a function of $g_0\tau_c$. (c) The lower bound of the mean-squared error as a function of g/g_0 .

in the experiment described in Ref. [31], the final state of the TLS leaving the cavity is detected with the help of a push-out laser. This method has the potential to perform the above

described inefficient measurement scenario. Furthermore, we have computed the average estimator and showed the biased nature of the obtained MMSE estimators. We have determined the lower bound of the mean-squared error with the help of a quantum Cramér-Rao-type inequality by constructing the symmetrized logarithmic derivative of the density matrix subject to estimation. These calculations have been performed for initial coherent field states. The increase of the initial mean photon number decreases the effectivity of the estimation scenario because a lot of information is deposited in the photon number states, which in turn are traced out to obtain the state of the TLS subject to the measurements. We have also found that the mean-square error estimation scenario is optimal, and our prior expectations are not reinforced, when the TLS emits a photon into the single-mode field with 50% probability. This is in contrast with many experimental situations, where every parameter is tuned such that every TLS emits a photon in the cavity, thus realizing the so-called one-atom maser [32].

In the case of the maximum-likelihood (ML) approach, the method used for the determination of the MMSE estimator cannot be applied. The observation strategy formulated with the help of the infinitesimal operators in Eq. (11) has led us to a pure mathematical problem. In general, the corresponding equations for the optimum strategy involving the risk operator are challenging to solve [4], but by constructing these infinitesimal operators with the help of square integrable functions, which form a Hilbert space with their respective inner product, we have been able to calculate the optimal POVMs. In the case of the Gaussian prior PDF the Hilbert space is $\mathbb{L}^2(\mathbb{R})$ with the orthonormal basis formed by Hermite polynomials. The Hilbert space for the uniform prior PDF case is $\mathbb{L}^2([-1, 1])$ with an orthonormal basis formed by sine and cosine functions. We have used the geometrical properties of these Hilbert spaces in order to optimize the average cost function. In order to be able to solve this problem, we have considered the detuning to be zero and the initial state of the field to be the vacuum state. Aside from the main result of determining the ML estimator and the optimized average cost function, we have shown that effects of spontaneous emission are again destructive and that long interaction times lead to inconclusive estimation scenarios. For both the Gaussian and the uniform *a priori* PDF, the POVM elements are diagonal in the basis of the qubit and as we have discussed in the case of the MMSE estimator one may implement such quantum measurements in experiments.

A few generic comments on all of the strategies presented throughout the paper are in order. The measurement data with the implemented POVM determines the average estimate or the *a posteriori* PDF from which one may infer the value of the matter-field coupling constant. The lower bound of the mean-squared error characterizes the accuracy, but we have found that better accuracy, defined in this way, is usually associated with inconclusive scenarios. Therefore, if we would like to compare the different methods then it has to be done through the average cost function. In this context, we can conclude that the choice of the uniform prior PDF is more suited for the model presented here, as shown in, e.g., Fig. 6. In the case of a Gaussian prior PDF and the MMSE estimator, we are able to compare the conclusions of Ref. [6] on the estimation of the optomechanical coupling with those ones obtained

here in this paper. It seems that this particular estimation strategy is optimal in the two different models, when the interaction time is not too long compared to one order of characteristic time periods of the systems. In general, this may suggest that exchange of too many excitations between the interacting systems entail a less favorable MMSE estimation scenario. A marked difference in the optomechanical system is the existence of a class of initial states, where the average minimum cost of error is reduced by the increase of the average excitation number of the initial state. This is not case for the matter-field system presented here.

In view of recent developments in quantum information protocols based on matter-field interactions, our work can be seen as the step before the real-world application of such protocols, establishing the tools for the optimal estimation of the dipole coupling strength. While we have not been able to solve completely all the problems related to the Bayesian approach in the context of matter-field interactions, our results already allow us to make several important observations,

which are crucial prior to the experimental implementation of any quantum information protocol.

In closing, we note that whereas our discussion has been framed exclusively in the language of cavity QED and the interaction between TLSs and electromagnetic cavity mode, our framework may be applicable more broadly. For example, in hybrid optomechanical systems where a bosonic mode (corresponding to the mechanical motion of a high-quality mechanical oscillator) is coupled to a TLS, the dynamics is governed by a Hamiltonian similar in structure to Eq. (1) [33,34]. The application of our techniques to this and similar scenarios is deferred to future work.

ACKNOWLEDGMENTS

This work is supported by the European Union's Horizon 2020 research and innovation programme under Grant Agreement No. 732894 (FET Proactive HOT).

-
- [1] J. Kaipio and E. Somersalo, *Statistical and Computational Inverse Problems*, Applied Mathematical Sciences Vol. 1 (Springer-Verlag, New York, 2005).
- [2] C. W. Helstrom, *Quantum Detection and Estimation Theory* (Academic Press, New York, 1976).
- [3] A. S. Holevo, *Probabilistic and Statistical Aspects of Quantum Theory* (North-Holland, Amsterdam, 1982).
- [4] A. Holevo, *J. Multivar. Anal.* **3**, 337 (1973).
- [5] C. W. Helstrom, *J. Stat. Phys.* **1**, 231 (1969).
- [6] J. Z. Bernád, C. Sanavio, and A. Xuereb, *Phys. Rev. A* **97**, 063821 (2018).
- [7] J. M. Raimond, M. Brune, and S. Haroche, *Rev. Mod. Phys.* **73**, 565 (2001).
- [8] N. Sangouard, C. Simon, H. de Riedmatten, and N. Gisin, *Rev. Mod. Phys.* **83**, 33 (2011).
- [9] W. P. Schleich, *Quantum Optics in Phase Space* (Wiley-VCH, Weinheim, Germany, 2001).
- [10] M. Brune, F. Schmidt-Kaler, A. Maali, J. Dreyer, E. Hagley, J. M. Raimond, and S. Haroche, *Phys. Rev. Lett.* **76**, 1800 (1996).
- [11] S. Gleyzes, S. Kuhr, C. Guerlin, J. Bernu, S. Deléglise, U. B. Hoff, M. Brune, J.-M. Raimond, and S. Haroche, *Nature (London)* **446**, 297 (2007).
- [12] L. Isenhower, E. Urban, X. L. Zhang, A. T. Gill, T. Henage, T. A. Johnson, T. G. Walker, and M. Saffman, *Phys. Rev. Lett.* **104**, 010503 (2010).
- [13] R. Demkowicz-Dobrzański, M. Jarzyna, and J. Kołodyński, in *Progress in Optics*, edited by E. Wolf (Elsevier, Amsterdam, 2015), Vol. 60, pp. 345–435.
- [14] M. Brunelli, S. Olivares, and M. G. A. Paris, *Phys. Rev. A* **84**, 032105 (2011).
- [15] M. Brunelli, S. Olivares, M. Paternostro, and M. G. A. Paris, *Phys. Rev. A* **86**, 012125 (2012).
- [16] I. Dobrakov, *Czech. Math. J.* **20**, 511 (1970).
- [17] K. Yosida, *Functional Analysis* (Springer-Verlag, Berlin, 1995).
- [18] L. Förster, W. Alt, I. Dotsenko, M. Khudaverdyan, D. Meschede, Y. Miroshnychenko, S. Reick, and A. Rauschenbeutel, *New J. Phys.* **8**, 259 (2006).
- [19] M. Khudaverdyan, W. Alt, I. Dotsenko, T. Kampschulte, K. Lenhard, A. Rauschenbeutel, S. Reick, K. Schörner, A. Widera, and D. Meschede, *New J. Phys.* **10**, 073023 (2008).
- [20] E. T. Jaynes and F. W. Cummings, *Proc. IEEE* **51**, 89 (1963).
- [21] H. Paul, *Ann. Phys.* **466**, 411 (1963).
- [22] S. D. Personick, *IEEE Trans. Inf. Theory* **17**, 240 (1971).
- [23] There are subtle differences between the mean-squared error, the variance of the estimator, and the variance of the mean-square error. An unfortunate combination of these words is used in our previous work, Ref. [6], to describe the one and the same thing (the mean-squared error). In fact, the mean-squared error is the sum of the variance and the squared bias of the estimator.
- [24] A. Perelomov, *Generalized Coherent States and Their Applications* (Springer-Verlag, Berlin, 1986).
- [25] Y. Colombe, T. Steinmetz, G. Dubois, F. Linke, D. Hunger, and J. Reichl, *Nature (London)* **450**, 272 (2007).
- [26] S. Ritter, Ch. Nölleke, C. Hahn, A. Reiserer, A. Neuzner, M. Uphoff, M. Mücke, E. Figueroa, J. Bochmann, and G. Rempe, *Nature (London)* **484**, 195 (2012).
- [27] M. Reed and B. Simon, *Methods of Modern Mathematical Physics I: Functional Analysis* (Academic Press, San Diego, 1980).
- [28] G. Dattoli, A. Renieri, and A. Torre, *Rad. Phys. Chem* **53**, 391 (1998).
- [29] L. Galué, *Math. Balkanica* **13**, 377 (1999).
- [30] M. Abramowitz and I. A. Stegun, *Handbook of Mathematical Functions* (Dover, New York, 1968).
- [31] S. Kuhr, W. Alt, D. Schrader, I. Dotsenko, Y. Miroshnychenko, W. Rosenfeld, M. Khudaverdyan, V. Gomer, A. Rauschenbeutel, and D. Meschede, *Phys. Rev. Lett.* **91**, 213002 (2003).
- [32] D. Meschede, H. Walther, and G. Müller, *Phys. Rev. Lett.* **54**, 551 (1985).
- [33] P. Rabl, P. Cappellaro, M. V. Gurudev Dutt, L. Jiang, J. R. Maze, and M. D. Lukin, *Phys. Rev. B* **79**, 041302(R) (2009).
- [34] K. H. Ng and C. K. Law, *Phys. Rev. A* **93**, 043834(R) (2016).